EXPERIMENTAL STUDIES
OF WEAK SUPERCONDUCTIVITY

Thesis by

Randall Keenan Kirschman

In Partial Fulfillment of the Requirements

for the Degree of

Doctor of Philosophy

California Institute of Technology

Pasadena, California

1972

(Submitted November 10, 1971)

ACKNOWLEDGEMENTS

This thesis owes its existence to the work of many people, to whom I acknowledge my indebtedness. Among these, I would like to specifically name the following people:

My adviser, Dr. J. E. Mercereau, who undertook the task of training me to become a scientist, who made constant suggestions and criticisms, who provided financial support, and who oversaw the development of an outstanding low-temperature physics laboratory.

Dr. Harris A. Notarys, who was always available as a source of advice, information, and assistance, day or night; who frequently put aside his own research to help me; who did more than his share in organizing and developing the laboratory; who did all this and more on a diet of Chandler Dining Hall cuisine.

Edward Boud and Sandy Santantonio, who made much of the equipment I used and taught me many secrets of their craft, who did the thousand everyday tasks without which the laboratory could not survive.

Dr. G. J. Dick, a font of ideas, assistance, wit, and apparatus.

Ed Kelm, who provided a great deal of help with the technical aspects.

Dr. G. Duthie and W. F. Baron, who helped with the mathematical analysis.

Fred Wild, craftsman and philosopher, who sharpened many a dull moment with an amusing story.

I would also like to thank the National Science Foundation and the California Institute of Technology for financial support that was essential to my work.

Finally, I would like to thank the North Holland Publishing Company, Amsterdam for permission to use figures 6-1, 7-1, and 7-3, which appeared in Physics Letters, Vol. 34A and 35A (1971).

ABSTRACT

Experimental investigations were made of the nature of weak superconductivity in a structure having well-defined, controllable characteristics and geometry. Controlled experiments were made possible by using a thin-film structure which was entirely metallic and consisted of a superconducting film with a localized section that was weak in the sense that its transition temperature was depressed relative to the rest of the film. The depression of transition temperature was brought about by underlaying the superconductor with a normal metal.

The DC and AC electrical characteristics of this structure were studied. It was found that this structure exhibited a non-zero, time-average supercurrent at finite voltage to at least .2 mV, and generated an oscillating electric potential at a frequency given by the Josephson relation. The DC V-I characteristic and the amplitude of the AC oscillation were found to be consistent with a two-fluid (normal current-supercurrent) model of weak superconductivity based on a thermodynamically irreversible process of repetitive phase-slip, and featuring a periodic time dependence in the amplitude of the superconducting order parameter.

The observed linewidth of the AC oscillation could be accounted for by incorporating Johnson noise in the two-

fluid model.

Experimentally it was found that the behavior of a short (length on the order of the coherence distance) weak superconductor could be characterized by its critical current and normal-state resistance, and an empirical expression was obtained for the time dependence of the supercurrent and voltage.

It was found that the results could not be explained on the basis of the theory of the Josephson junction.

TABLE OF CONTENTS

I. INTRODUCTION

When the flow of electric current in metals was first studied in the early nineteenth century, it was found that an electric current flowing between two points in a metal always required an electric potential difference between those two points: the metal was said to be resistive. It was found later that an explanation for this behavior was that the current carrying, or conduction, electrons in a metal do not accelerate continuously, but undergo collisions with the metal ions and lose their kinetic energy. Consequently, current flow in a metal would be accompanied by dissipation of electric power.

During the late nineteenth century there was considerable progress in reaching low temperatures, but it was not until after 1908, when Onnes first liquified helium and used it as a refrigerant, that the electrical behavior of metals was studied at temperatures within a few degrees of absolute zero. In the course of a few years Onnes had discovered that, for certain metals, as the metal was cooled, there was a temperature at which its resistance abruptly dropped to a value lower than he could measure (London 1950, Lynton 1969). Since then, attempts to determine this resistance have had the result that it is immeasureably small when measured under conditions of

thermodynamic equilibrium and in the steady state (File and Mills 1963), and its value is believed to be exactly zero.

This situation, in which a metal exhibits zero resistance, is called the superconducting state. The resistive state of metals mentioned earlier is called the normal state. Metals exhibiting superconductivity at low temperature, for example tin and niobium, are called superconductors. There are other metals, for example gold and copper, that are always in the normal state, so far as is known; these are called non-superconductors.

It was found that the superconducting state was not merely a state of zero resistance, but that it exhibited the ability to expel an externally applied magnetic field. This phenomenon of field expulsion, known as the Meissner effect, cannot be explained on the basis of perfect conductivity (Lynton 1969).

In addition, it was found that if the magnetic field exceeded a certain value, called the critical field, H_c, superconductivity would be destroyed. For a given metal, the critical field was found to depend on temperature, being a maximum, $H_c(0)$, for $T = 0$ and decreasing to zero as the temperature increased to T_c, the critical temperature of the metal.

To indicate the typical magnitude of these parameters, tin has $T_c = 3.72\ ^oK$, $H_c(0) = 306$ gauss, and niobium has $T_c = 9.46\ ^oK$, $H_c(0) = 1944$ gauss (Lynton 1969).

Understanding the nature and origin of superconductivity took many years. In part this was due to experimental difficulties, but primarily it was due to the difficulty of arriving at a successful microscopic theory.

About 20 years after the discovery of superconductivity it was established that the superconducting state could be regarded as a thermodynamic equilibrium state and that the transition between the superconducting and normal states (either in the presence or absence of a magnetic field) was a reversible thermodynamic phase transition. A number of phenomenological theories of superconductivity were developed at about the same time, many of which have not lost their usefulness.

It was not until 1957 that a microscopic theory was developed, by Bardeen, Cooper and Schrieffer (1957a,b), that accounted for all the essential phenomena of superconductivity. An important consequence of this theory was that in a superconductor the conduction electrons could be considered to be in a single highly-ordered quantum state in which their motion is correllated and collissionless.

Recently, it has been found that superconductivity,

and supercurrents, can also exist in situations of non-equilibrium (Anderson 1966). One such situation is a type of superconductivity known as weak superconductivity, which occurs in a structure that is entirely superconducting, referred to as a weak superconductor. A weak superconductor may be resistive, in the sense that a supercurrent may be accompanied by a finite potential and dissipation of power. In addition, a weak superconductor can produce oscillating electric currents and potentials, whose frequency of oscillation has been found to extend at least as high as 10^{10} sec^{-1}. It will be shown that these effects may be explained by assuming a periodic time-dependence in the strength of the superconducting state in a weak superconductor. All experimental evidence indicates that these phenomena are confined to superconductors of small size, volumes typically being on the order of 10^{-9} cm^3.

Weak superconductivity should not be confused with the Josephson effect, another situation in which oscillating currents and potentials arise from a time-dependent superconductivity. This effect occurs in the Josephson, or insulating, junction, which consists of two superconductors separated by an insulator which is thin enough to allow coupling (Josephson 1962). This type of superconductivity

is intrinsically thermodynamically reversible and non-dissipative, (except in certain junctions in the case of large supercurrent, where a dissipative mechanism may come into play (Clarke 1971)).

In the Josephson junction, however, the time-dependence is not in the strength of the superconducting state, but in its quantum-mechanical phase. Thus, the Josephson junction is not a weak superconductor as the term is used here. In spite of their basic differences, there are many similarities between the Josephson junction and the weak superconductor, which might lead one to attempt an interpretation of the phenomena of weak superconductivity in terms of the theory of the Josephson junction. However, such an approach must prove inadequate because of the fundamental differences between the two structures in their operation and behavior, which will be discussed further.

Since its discovery, notable advances have been made in understanding weak superconductivity; however, there is still much to be learned about the physical basis of weak superconductivity, the characteristics of weak superconductivity and how it differs from other physical situations, and how a weak superconductor interacts with external fields.

The research discussed in this thesis represents an effort to gain a better understanding of weak superconductivity along these lines, by means of a program of experiments involving a thin-film structure in which, as will be shown, there is reason to believe weak superconductivity exists.

Specifically, the following characteristics of this structure were investigated: (1) Its low and high frequency electrical behavior, (2) The effect of an external magnetic field and the effect of external electromagnetic radiation, (3) The effect of varying its geometry. From the information obtained, a model has been devised and, we believe, a better understanding of weak superconductivity has been attained.

A summary of some of the work presented in this thesis has appeared in two publications (Kirschman, Notarys, and Mercereau 1971, Kirschman and Mercereau 1971).

II. PHYSICAL BACKGROUND

The electrons in a metal, whether normal or superconducting, are governed by Fermi statistics, which requires that each occupy a different quantum state.

2-1 Normal State.--First, consider a metal in the normal state. In a rudimentary description the conduction electrons fill the states within a sphere in 3-dimensional momentum space, referred to as the Fermi sphere (Kittel 1971). At finite temperature momentum is continually transferred between individual electrons and the lattice through collisions, which tends to keep the sphere centered at the origin. In the absence of an electric current the sphere remains centered at the origin--its net momentum is zero.

An electric field applied to the metal adds momentum to the electrons and displaces the sphere from the origin, which represents a net current proportional to the displacement, and the sphere attains an equilibrium displacement such that the rate at which net momentum is lost to the lattice through collisions equals the rate at which net momentum is gained from the electric field. Thus an electric field is necessary to maintain this displacement, and it turns out that the displacement of the sphere, and consequently the current, are proportional to the electric

field--this relationship is known as Ohm's law. The proportionality is strictly true only for small currents--which is the case in practice.

In the normal state the motion of the electrons is uncorrelated and the available energy levels are closely spaced, thus arbitrarily small excitations are possible, allowing a continuous loss of momentum and energy through collisions with the lattice, which makes current flow in the normal state dissipative. If the electric field is removed, the sphere, and current, relax to zero in a time given by

$$\tau = \frac{m\sigma}{ne^2} \qquad (2\text{-}1)$$

where n is the number density of electrons and σ is the conductivity (Kittel 1971). This relaxation time, τ, may be on the order of 10^{-9} seconds or less.

A related parameter is the mean free path, Λ, which is the average distance an electron travels between collisions, and is given by

$$\Lambda = v_F\tau = \frac{v_F m}{ne^2}\sigma \qquad (2\text{-}2)$$

where v_F, the Fermi velocity, is the velocity at the surface of the Fermi sphere. The appropriate velocity is v_F because only electrons at the Fermi surface participate

in dissipative collisions with the lattice.

2-2 Superconducting State.--Now consider the superconducting state. The following description applies to weak or strong superconductivity in general. Although electrons in the superconducting state are still governed by Fermi statistics, they may be considered to all be in the same quantum state. The justification for such a simplifying assumption comes from the Bardeen, Cooper, and Schrieffer (1957a,b) (BCS) theory of superconductivity.

This theory first demonstrated that under the proper circumstances, in a system of conduction electrons and lattice, there can be an attractive interaction between two electrons having exactly opposity momentum and spin, which dominates the coulomb repulsion, and leads to a net lowering of energy of the system. The mechanism shown to mediate this interaction is the exchange of lattice phonons (quantized vibrations of the ionic lattice) between the two electrons; however, additional mechanisms have also been suggested (Matthias 1960). Attempts to determine the occurence and size of this interaction in various materials so far have not been successful.

Since the phonon energy is always very much less than the energy of an electron near the surface of the Fermi sphere, only electrons in a narrow shell at the Fermi

surface can participate in this interaction. The greatest lowering of energy would occur when conditions were such that there would be the largest number of interactions possible to form opposite-momentum pairs of electrons. This situation prevails if all pairs have exactly the same center-of-mass momentum. Therefore, in the BCS theory it is hypothesized that the superconducting state is a highly ordered one in which (at $0^{\circ}K$) as much as possible, electrons near the Fermi surface occupy states in pairs with opposite momentum and spin.

A further consequence of the theory is that the system has a single ground state--the BCS ground state. An excitation made by removing a superconducting electron from a state with momentum p not only destroys the pair (p,-p) of which it is a member, but also eliminates a large number of pairs which could have interacted to occupy the states with momentum p and -p. Thus any excitation raises the energy of the system by a comparatively large amount, which means that the ground state is separated by a finite energy gap from the excited states. The size of the energy gap, $\Delta(T)$, which is temperature dependent, is given by the theory (Lynton 1969). At $0^{\circ}K$ it is

$$\Delta(0) \approx 3.5\ kT_c \qquad (2\text{-}3)$$

A typical critical temperature, T_c, of 4° K gives an energy gap, $\Delta(0)$, of about 1.4 meV. The gap $\Delta(T)$ decreases with increasing T, vanishing at T_c.

A current flow in a superconductor--a supercurrent--corresponds to a displacement of the Fermi sphere as in the normal state. However, the energy gap makes it extremely unlikely for momentum and energy to be lost through collisions and the supercurrent does not require an electric field to sustain it. Current flow in a superconductor is thus a metastable state which experiments have shown has a relaxation time greater than 3×10^{12} seconds (100,000 years) (File and Mills 1963).

On the basis of the BCS theory, if all electron pairs have the same center-of-mass momentum, then the motion of the electrons is correlated over macroscopic distances and they behave as though they were in a single quantum state, referred to as the macroscopic quantum state. The wavefunction of this state may be represented as

$$\Psi(\vec{r},t) = a(\vec{r},t)e^{i\theta(\vec{r},t)} \qquad (2\text{-}4)$$

where the amplitude, $a(\vec{r},t)$ and the phase, $\theta(\vec{r},t)$ are chosen to be real functions of position, r, and time, t (Feynman, Leighton, and Sands 1965).

2-3 Coherence Distance.--The energy associated with the wavefunction Ψ contains a term that is proportional to

the integral of $(\partial \Psi/\partial x)^2$, so any spatial variation in Ψ increases the energy. Thus, it might be expected that to preserve superconductivity spatial variations of ρ and θ cannot be too rapid, or the additional energy would make the superconducting state thermodynamically unfavorable with respect to the normal state. The BCS theory confirms this expectation, and gives a minimum distance, ξ, over which the wavefunction can vary drastically.

The following dimensional argument gives a correct estimate for ξ_0, the coherence length in most pure metals without imperfections, where the electronic mean free path, Λ, is large compared to ξ_0. At the Fermi surface a change in energy of Δ corresponds to a change in momentum of $\Delta p=(m/p_F)\Delta$, where p_F is the momentum at the Fermi surface and is equal to mv_F. Thus $\Delta p = \Delta/v_F$. The uncertainty relation is used to convert Δp into the length ξ_0, and thus

$$\xi_0 = \frac{\hbar v_F}{\Delta} \qquad (2\text{-}5)$$

Using the typical values Δ = 1 meV, and $v_F = 10^8$ cm/sec (Kittel 1971) gives $\xi_0 \approx 10^{-4}$ cm.

For superconductivity in impure metals, alloys, and certain pure metals where $\Lambda \ll \xi_0$, collisions tend to disrupt the superconducting state and the coherence length is given

by

$$\xi \approx .8\sqrt{\xi_0 \Lambda} \qquad (2\text{-}6)$$

(De Gennes 1966).

2-4 Macroscopic Quantum State.--Although the wavefunction Ψ has the same form as a single electron wavefunction it may be interpreted in a different way. If Ψ were the wavefunction of a single electron then $|\Psi|^2 dV$ would be the probability of finding the electron in the small volume dV. If the volume dV were examined once, the electron would either be there--giving a charge e, or would not be there--giving a charge 0. If the average were taken of many examinations the result would be an average charge equal to $e|\Psi|^2$. In the case of the macroscopic quantum state, where many electrons are in the same state described by $\Psi, |\Psi|^2 dV$ is the probability of finding any one of many electrons in the volume dV, and one examination is the eqivalent of making many examinations in the preceeding case. Thus the probability density $|\Psi|^2$ of the macroscopic quantum state, Ψ, of superconductivity may be identified as the electric charge density ρ. Therefore, let

$$a(\vec{r},t) = \sqrt{\rho(\vec{r},t)} \qquad (2\text{-}7)$$

and

$$\Psi(\vec{r},t) = \sqrt{\rho(\vec{r},t)}\, e^{i\theta(\vec{r},t)} \qquad (2\text{-}8)$$

It has been found that an electron may be decribed as a wave packet. In such a case it would seem reasonable to expect the evolution of this wave packet, which would give the motion of the electron, to be described by a wave equation. It turns out that this is the case and that the appropriate wave equation is the Schroedinger equation (Eisberg 1961).

It is assumed here that the same Schroedinger equation can be applied to the macroscopic quantum state of superconductivity, which arises from a large number of electrons, in other words that the wavefunction describing the macroscopic quantum state may be substituted into the Schroedinger equation, which is

$$-\frac{\hbar}{i}\frac{\partial\Psi}{\partial t} = \frac{1}{2m}\left(\frac{\hbar}{i}\nabla - qA\right).\left(\frac{\hbar}{i}\nabla - qA\right)\Psi + q\phi\Psi \qquad (2\text{-}9)$$

(Feynman, Leighton, and Sands 1965). Substituting (2-8) into the equation and equating real and imaginary parts of both sides yields for the imaginary part

$$m\frac{\partial\rho}{\partial t} = \hbar\vec{\nabla}\theta\cdot\vec{\nabla}\rho + \rho\nabla^2\theta - \frac{q}{m}\vec{A}\cdot\vec{\nabla}\rho + \rho\vec{\nabla}\cdot\vec{A} \qquad (2\text{-}10)$$

and for the real part

$$\hbar\frac{\partial\theta}{\partial t} = -q\phi - \frac{\hbar^2(\nabla\theta)^2}{2m} + \frac{\hbar^2}{2m}\left(\frac{1}{\sqrt{\rho}}\nabla^2\sqrt{\rho}\right) - q^2A^2 - 2q\hbar\vec{A}\cdot\vec{\nabla}\theta \qquad (2\text{-}11)$$

In the presence of current sources and sinks, the supercurrent density $\vec{j}_s$ will be of interest. It is related to ρ by the continuity equation,

$$\frac{\partial \rho}{\partial t} = \nabla \cdot \vec{j}_s \tag{2-12}$$

It turns out that the right hand side of (2-10) is a perfect divergence and thus

$$\vec{j}_s = \frac{\rho}{m} \hbar \vec{\nabla} \theta - \frac{q}{m} \rho \vec{A} \tag{2-13}$$

It can be seen that any constant independent of $\vec{r}$ and t added to θ will not affect the experimentally observable variables $\vec{j}_s$ and ρ. Only differences in θ between two points can be determined. This indeterminacy in θ just means that there is an arbitrary phase factor in Ψ.

Because there is a minimum distance, ξ, in a superconductor, the relations given above are not local ones relating the variables at a point: averages over distances on the order of ξ must be made. In order to comply with this restriction, all distances over which the variables change will be assumed large compared to ξ in what follows.

Now apply these results to a superconducting wire (or film), of cross section, s, small enough that it may be considered "one-dimensional," in the sense that the only variation of ρ and θ is along the length of the wire--which is chosen to be the x axis. The criteria which

insure one-dimensionality will be discussed later. Suppose the wire is of length L and that the ends are connected to boundary pieces of strong superconductor at $x \leq 0$ and $x \geq L$; "strong" meaning that the superconducting density is large enough to be considered constant in the boundary pieces for the currents considered here.

Let $\delta\theta$ be the phase difference between the ends of the wire:

$$\delta\theta \equiv \int_0^L \nabla\theta d \qquad (2\text{-}14)$$

2-5 Supercurrent States.--Suppose a supercurrent j_s flows through the wire. For convenience the gauge in which zero magnetic field corresponds to $\vec{A} = 0$ will be used. Suppose also that the magnetic effects from the supercurrent j_s can be neglected: the justification for this assumption will be given later. Then from (2-13)

$$I_s = sj_s = \frac{s\rho\hbar}{m}\frac{\delta\theta}{L} \qquad (2\text{-}15)$$

Now consider the phase difference, $\Delta\theta$, evaluated only at the ends of the wire: $\Delta\theta \equiv \theta(L) - \theta(0)$. Since the phase is periodic in 2π, this phase difference, $\Delta\theta$, is indeterminate by $2\pi n$ and does not uniquely determine $\delta\theta$,

or the supercurrent j_s. Thus for any boundary condition on $\Delta\theta$ there corresponds an infinite number of current states, differing in supercurrent by

$$\Delta I_s = \frac{\rho hs}{mL} \tag{2-16}$$

2-6 Potential Difference.--Equation (2-11) may be applied by evaluating the variables in the boundary pieces at 0 and L, again taking $\vec{A} = 0$. This gives

$$\hbar(\theta_L-\theta_0) = -q(\phi_L-\phi_0) - \frac{\hbar^2}{2m}(\nabla\theta)^2\Big|_0^L + \frac{\hbar^2}{2m}\left(\frac{1}{\sqrt{\rho}}\nabla^2\sqrt{\rho}\right)\Big|_0^L \tag{2-17}$$

In the boundary pieces ρ is constant so the last term can be neglected. Likewise, since $j_s \propto \rho\nabla\theta$ and j_s is equal in the two boundary pieces, the third term may also be neglected. In general, for instance in the middle of the wire, the last two terms cannot be neglected. They can be neglected here only by virtue of the special, but not unrealistic, boundary conditions imposed. Thus

$$\hbar(\dot{\delta\theta}) = -qV \tag{2-18}$$

where $(\dot{\delta\theta}) = \dot{\theta}_L-\dot{\theta}_0$ from (2-14) and $V \equiv \phi_L-\phi_0$ is the electric potential difference between the ends of the superconducting wire.

It has been found (Feynman, Leighton, and Sands 1965,

De Gennes 1966, Lynton 1969) that the appropriate value for q is -2e, which indicates that superconducting electrons act in pairs, in some sense, in accord with the pairing interaction in the BCS theory and the occurrance of the quantity 2e in the flux quantum, $\Phi_o = h/2e$. Thus

$$\hbar(\delta\dot{\theta}) = 2eV \qquad (2\text{-}19)$$

Therefore, if a potential difference, V, exists between the ends of the wire, the phase difference must increase monotonically in time according to equation (2-15). Note that this is just the result expected classically on the basis of a collisionless group of electrons in an electric field.

2-7 Instabilities in Superconductors.--However, the process of increasing supercurrent cannot contine indefinitely, because eventually a current will be reached which is large enough to destroy superconductivity. This comes about when the quantum phase, θ, goes through a period of 2π in a distance comparable to ξ.

A more complete description is as follows: A consequence of the BCS theory (Bardeen 1962, Schmid 1969) is that the density of superconducting electrons, ρ, decreases with increasing momentum p and vanishes for $p \geq p_c \approx \frac{\hbar}{\xi}$ (refer to section 2-3 where Δp was used for p_c).

Because the supercurrent, j_s, is proportional to

ρp, j_s as a function of p increases from zero through a maximum, j_m, at p_m and falls to zero for $p = p_c$. The re-tion $p_m<p<p_c$ is unstable (Schmid 1969) and in this region j_s decays spontaneously and rapidly to zero. It turns out that $p_m = p_c/\sqrt{3}$ (Bardeen 1962). Thus the maximum super-current, j_m, flows when

$$\frac{\delta\theta}{\Delta x} = \frac{p_m}{\hbar} = \frac{1}{\sqrt{3}\xi} \qquad (2\text{-}20)$$

2-8 Transitions Between States.--One way that the wire can remain superconducting with a potential across it is by means of a mechanism that reduces the phase differ-ence $\delta\theta$, and thus the supercurrent, j_s, as required by equation (2-19). This can come about through a transition from a high current state to a lower one which also satis-fies the boundary condition on $\Delta\theta$. Such a process in which the phase $\delta\theta$ and current j_s change will be referred to as "phase slip."

Suppose $L \approx 2\pi\sqrt{3}\xi \approx 10\xi$, then from equation (2-20) the maximum $\delta\theta$ will be 2π, and the maximum I_s (the criti-cal current) will be ΔI_s from equations (2-15) and (2-16). The next lower current state will be $\delta\theta = 0$, $j_s = 0$. In this case the phase can slip only by 2π.

Now consider the general case $L \approx n2\pi\sqrt{3}\xi$. The maximum, or critical, supercurrent I_{sc} is $n\Delta I_s$ and there are n+1 supercurrent states (including $I_s = 0$) in all.

Thus the phase can slip by 2π, 4π, ..., $2\pi n$.

It was possible to describe the weak superconductor during the process of increasing supercurrent by assuming that at each moment it was in thermodynamic equilibrium--that the process was a succession of equilibrium current states.

The phase-slip process--a transition between equilibrium states--is not itself an equilibrium process and thus cannot be described by the equations used above. So far, no analytical treatment of the phase-slip process exists; however, it is still possible to arrive at some conclusions regarding it.

2-9 Energy.--It is possible to get an estimate of the energy difference between current states. Associated with each state is a potential energy which is the same for each state and a kinetic energy K which may be estimated as

$$K = \int_0^L \frac{1}{2} m v_s^2 \frac{\rho_s}{e} \approx \frac{1}{2} m v_s^2 \frac{\rho_s}{e} L \quad (2\text{-}21)$$

Using (2-15) gives

$$K \approx \frac{1}{2} \frac{mL}{\rho_{es}} I_s^2 \quad (2\text{-}22)$$

The difference in energy between adjacent states, i and f, is thus

$$\Delta K \approx \frac{1}{2} \frac{mL}{\rho_{es}} (I_{si}^2 - I_{sf}^2) \quad (2\text{-}23)$$

$$\Delta K \approx \frac{1}{2}\frac{h}{2e}(I_{si} - I_{sf}) \quad \text{or} \quad \Delta K \approx \frac{1}{2}\Phi_0(I_{si} + I_{sf}) \qquad (2\text{-}24)$$

where the relation $I_{si}-I_{sf}=\Delta I_s=\frac{\rho h}{mLs}$ from equation (2-16) was used. A similar result has been obtained from the Ginzburg-Landau theory of superconductivity (Langer and Ambegaokar 1967).

2-10 Kinetic Inductance.--It is well known that there is an inductance due to the fact that an electric current creates a magnetic field. This inductance will be referred to as the magnetic inductance, $\mathcal{L}_M$. Any change in the current, I, through an inductance $\mathcal{L}_M$ is accompanied by a voltage $V = \mathcal{L}_M \frac{dI}{dt}$. This reflects the fact that electric power, VI, must be supplied to change the energy in the magnetic field created by the current, I. The current has an "inertia"--it takes energy to change the value of the current.

In a superconductor there is another inductance, in addition to the magnetic inductance, which will be referred to as the kinetic inductance, $\mathcal{L}_K$. The kinetic inductance arises from the fact that any supercurrent flow causes a spatial variation of θ and thus increases the energy of the superconducting state--changing the supercurrent requires energy. To obtain the value of $\mathcal{L}_K$, equations (2-15) and (2-19) give the following time-dependent relationship between V and j_s

$$V \approx \frac{mL}{2e\rho s}\frac{dI_s}{dt} \qquad (2\text{-}25)$$

thus

$$\mathcal{L}_K \approx \frac{mL}{2e\rho s} . \qquad (2\text{-}26)$$

Kinetic inductance may be thought of as the mechanical inertia of the superconducting electrons--which behave as free particles. Roughly speaking, the electrons have an energy that depends quadratically on their velocity--and thus also depends quadratically on the supercurrent.

In reality the kinetic inductance is not independent of the magnitude of the supercurrent, especially for supercurrents close to the critical current (j_m), due to the non-linear dependence of j_s on p (section 2-7).

The kinetic inductance may be related to experimentally measurable quantities by expressing it as

$$\mathcal{L}_K = \frac{mL}{2e\rho s} = \left(\frac{h}{2e}\right)\left(\frac{\sqrt{3}\,\xi m}{\hbar \rho s}\right)\left(\frac{L}{2\pi\sqrt{3}\xi}\right) \qquad (2\text{-}27)$$

From section 2-7

$$j_c = \frac{\hbar \rho}{\sqrt{3}\xi m} \qquad (2\text{-}28)$$

thus

$$\mathcal{L}_K = \left(\frac{h}{2e}\right)\left(\frac{1}{j_c s}\right)\left(\frac{L}{2\pi\sqrt{3}\xi}\right) \qquad (2\text{-}29)$$

$$\mathcal{L}_K = \frac{\Phi_o}{I_c}\left(\frac{L}{2\pi\sqrt{3}\xi}\right) \qquad (2\text{-}30)$$

For the superconducting structures considered here it will be shown that the kinetic inductance is larger than the magnetic inductance when the requirements of one-dimensionality are satisfied.

2-11 Penetration Depth.--If a superconductor is placed in a magnetic field, the field penetrates a short distance into the surface. The approximate behavior can be obtained from equation (2-13) with $\nabla\theta = 0$ and the equation

$$-\mu j_s = \nabla^2 A \qquad (2\text{-}31)$$

from electromagnetic theory (Jackson, 1962). The solution of these equations is that inside the superconductor the field and supercurrent decay exponentially with distance from the surface. The decay constant is called the penetration depth, λ, and is given by

$$\lambda^2 = \frac{m}{\rho e \mu} \qquad (2\text{-}32)$$

This result was first given by London and London (1935) using a different line of reasoning. The penetration depth of a superconductor, λ, is temperature dependent, approaching ∞ as T approaches the critical temperature of the superconductor, since ρ is vanishing. The exact temperature dependence is

$$\lambda(T) \propto (T_c/\Delta T)^{\frac{1}{2}} \qquad (2\text{-}33)$$

where $\Delta T \equiv T_c - T$ (De Gennes 1966). In addition, in "dirty" metals, with $\Lambda \ll \xi_0$, λ is increased by the factor $(\xi_0/\Lambda)^{\frac{1}{2}}$ (De Gennes 1966).

2-12 Flux Quantization.--Suppose that a closed path is taken in a bulk superconductor, far enough (many penetration depths) inside that the currents are negligible. Then the condition $j_s = 0$ on equation (2-13) coupled with the facts that $\oint \nabla\theta = 2\pi n$ (n an integer) and $\oint A = \varphi$, implies $\varphi = nh/2e$. That is, for any closed path lying entirely in superconductor, the flux is quantized in units of $\varphi_0 \equiv h/2e \approx 2 \times 10^{-7}$ gauss-cm^2 (Byers and Yang 1961, Parks and Little 1964). Note that if $n \neq 0$ then there must be a singularity in the superconductor: a hole, or a normal spot where the field penetrates called a "vortex" (De Gennes 1966, Lynton 1969).

2-13 Josephson Junction.--Because the Josephson junction exhibits behavior similar to that of a weak superconductor, it will be referred to occasionally and a brief description will be given here as background.

The Josephson junction (Josephson 1962) consists of two superconductors separated by an insulating barrier which is thin enough to allow coupling.

The situation may be described by two macroscopic quantum states--one for each superconductor--and two

coupled Schroedinger equations. The solution of these equations is

$$\frac{d}{dt}(\theta_1-\theta_2) = \frac{2eV}{\hbar} \tag{2-34}$$

$$j_s = j_o \sin\left(\theta_1-\theta_2 + \frac{2e}{\hbar}\int_1^2 \vec{A}\right) \tag{2-35}$$

where j_o is a constant with the dimensions of a current density, whose magnitude depends on the strength of the coupling, and subscripts 1 and 2 refer to the two superconductors.

Thus for $V = 0$, the supercurrent j_s in a Josephson junction is constant with respect to time and is proportional to the difference in phase between the two sides of the junction. For $V \neq 0$ the phase difference increases with time and the supercurrent oscillates.

The term in the vector potential $\vec{A}$ reflects the fact that the supercurrent in the junction depends on the magnetic field, which causes the Josephson junction to exhibit a modulation of critical current in an applied field. In the junction, supercurrents which cross the insulating barrier by different paths in the presence of a magnetic field interfere with one another to produce this modulation as shown by the following analysis.

Let the barrier lie in the y-z plane, so that the supercurrent flows in the x-direction. The supercurrent at any point (y,z) depends upon the integral of the mag-

netic vector potential across the barrier at that point according to equation (2-35). Thus in the absence of a magnetic field the supercurrent density, j_s, is the same for all points (y,z) and the maximum, or critical, current is j_o times the area of the junction.

In the presence of a magnetic field, A_x varies in the y-z plane, and due to the sine dependence of j_s on A_x, the magnitude of the current density varies sinusoidally in the y-z plane. When the current density is integrated over the y-z plane to obtain the critical current, the currents at different points interfere. Thus, the critical current of the junction has a periodic dependence on the magnetic field.

The effect is analogous to the Fraunhofer diffraction of light passing through a slit, and gives the same interference pattern. It is important to note that the minima in the critical current as a function of B are not all equally spaced: the two minima about B = 0 are twice as far apart as the others.

III. MODELS OF WEAK SUPERCONDUCTIVITY

3-1 Repetitive Phase Slip.--A possible model of weak superconductivity is that the supercurrent at finite voltage results from a process of repetitive phase-slip, at an average rate which satisfies equation (2-19):

$\dot{\delta\theta}/2\pi = V/\Phi_0$.

One crude way of visualizing the process of phase-slip is the following: Imagine that ρ and θ are plotted in polar coordinates, with the x-axis as the polar axis, as shown in figure 3-1.

For a superconductor with $I = 0$, ρ is constant and θ may be set equal to zero from 0 to L. If a voltage is applied the (ρ,θ) line "winds up" into a helix around the x-axis as shown in figure 3-1a. When the helix becomes "tight" enough--I equals the critical current--one of the loops untwists by passing through the x-axis, and a lower current state is reached--the phase has "slipped" (figure 3-1b). This process of winding up and losing a loop repeats as long as there is a voltage. The process may be thought of as a type of relaxation oscillation in which the supercurrent builds up and decays repetitively.

For long structures ($L \gg \xi$) there would be many loops along the length of the weak superconductor, which could introduce randomness in the phase-slip process, in that

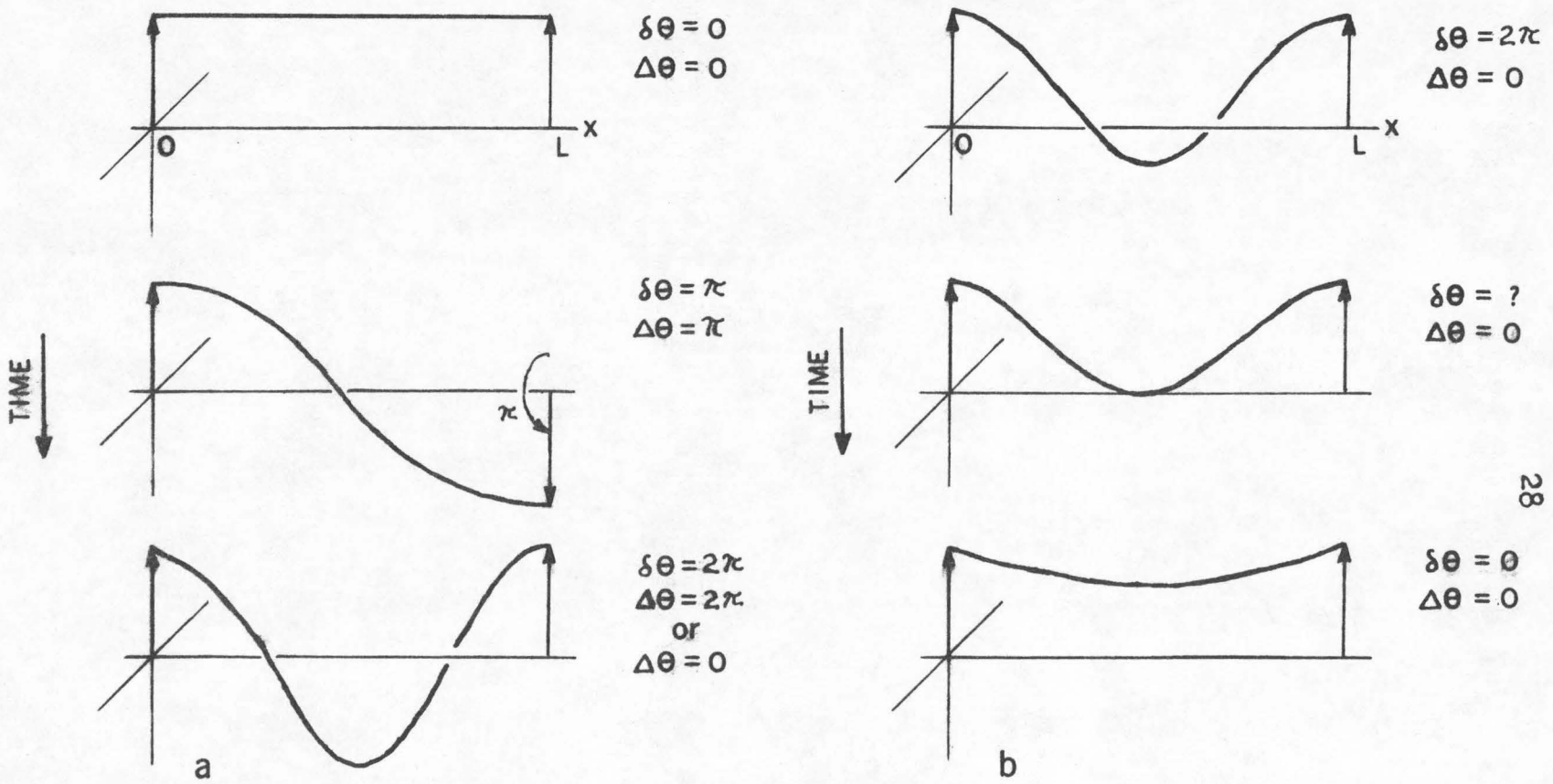

Fig. 3-1. Plots of ρ and θ versus x in a short ($L \approx 10\xi$) weak superconductor. (a) "winding up"--$\delta\theta$ increases, (b) phase-slip transition from higher to lower current state--$\delta\theta$ decreases by 2π (it is assumed that $\Delta\theta$ has not appreciably increased during the transition).

any one of the loops, or more than one loop, could be lost during a phase slip. For short structures $L \approx 10\xi$, however, only one loop would be allowed for $I \leq I_c$, which would eliminate randomness from the causes given above.

In order to wind up the helix and go from a lower to a higher current state, energy must be supplied to the weak superconductor according to equation (2-24). If it is assumed that the energy associated with the supercurrent is dissipated (for instance as heat or electromagnetic radiation), then to sustain the process of phase slip would require that power be supplied to the weak superconductor.

This picture of the phase-slip process in a voltage-supporting weak superconductor as a thermodynamically irreversible cycle is the origin of the idea that it is a time dependence in the amplitude of the order parameter which is responsible for the dissipation in a weak superconductor.

In contrast, since the average supercurrent in the Josephson junction is zero (equation 2-35), the junction is intrinsically reversible and non-dissipative. In a real Josephson junction there is dissipation due to dielectric loss in the barrier, electromagnetic radiation, or flux flow (section 3-3).

3-2 Two-Fluid Model.--In order for the helix to lose a loop and the phase to decrease, ρ must go to zero momentarily over a distance of at least ξ, which means that superconductivity is destroyed in a short section of the weak

superconductor. However, the adjacent parts of the wire remain superconducting and tend to restore superconductivity where the slip has occurred (see Langer and Ambegaokar 1967, Little 1967).

This picture suggests a "two-fluid" (normal current and supercurrent) model, in which there is a normal current I_n equal to $\langle V \rangle / R$, where $\langle V \rangle$ is the time-average voltage applied to the weak superconductor, and R is its effective resistance; and a supercurrent, I_s, which oscillates between 0 and I_c, and whose time-average value, $\langle I_s \rangle$, lies between 0 and I_c. The total current, I, equals $I_n + I_s$. Thus, when the weak superconductor is driven by a current source, a change in the supercurrent as it oscillates is compensated by a change in the normal current (ΔI_n). This model thus predicts an oscillating potential

$$v \approx \tfrac{1}{2}\Delta I_n R \approx \tfrac{1}{2} I_c R \qquad (3\text{-}1)$$

for phase-slip by 2π.

3-3 Flux Flow.--There is another mechanism that could accomplish the reduction in phase required if a superconductor is to support a voltage. This mechanism involves a motion of vortices (section 2-12) known as "flux flow" (Strnad, et al 1964, Tinkham 1964, Volger, et al 1964, Kim, et al 1965).

If a superconducting wire (or film) is carrying a great enough current, a quantum of flux--a "vortex"-- may

penetrate one side of the wire and be driven across by the Lorentz force to emerge on the opposite side, bringing about a reduction in phase between the ends of the wire of 2π. If only one quantum of flux is in the wire at a time the potential developed by this process will consist of pulses generated at a rate $\nu = \langle V \rangle / \Phi_0$ in accord with equation (2-19). The height and width of the pulses depend on the details of the flux flow process, but their integrated area must be $\langle V \rangle \nu$. If the pulse width is short compared to the time between pulses ($1/\nu$), then Fourier analysis gives the root-mean-square (RMS) amplitude of the first AC component at the frequency ν as

$$V_{RMS} = \sqrt{2}\langle V \rangle \qquad (3\text{-}2)$$

IV. DESCRIPTION OF SUPERCONDUCTING SAMPLES

To study weak superconductivity it was necessary to have a structure--in which the phenomenon existed--whose parameters could be varied over a wide range in a controllable manner, and which would give reproducible results.

In addition, from the standpoint of experimental convenience, it was desired that this structure be easy to fabricate, and be mechanically rugged and stable.

A superconducting structure was developed (Frieberts-hauser, et al 1968, Clarke 1970) with these requirements in mind and was found to meet them to a high degree. This structure will be referred to as the NM (Notarys-Mercereau) structure.

"Weak" in reference to weak superconductivity is a relative term, which means that in a weak superconductor the density of superconducting electrons ρ , is small relative to ρ in a "strong" superconductor.

4-1 Weakening.--In the NM structure the weakening is brought about in a thin film of superconductor (with transition temperature T_c) by depressing the transition temperature to $T_c' < T_c$ in a localized region.

The superconducting electron density ρ in a superconductor is strongly dependent on temperature, T, being maximum for T = 0 and approaching zero as T increases to

the critical temperature. Thus if T_c' is significantly less than T_c there will be a range near T_c' where the localized region is weak compared to the main film, as required.

In the NM structure the transition temperature is depressed in the localized region by a material inhomogeniety. This allows the superconductivity to be weakened without mechanically weakening the film.

In these structures the transition temperature is depressed in a controllable manner by underlaying the superconducting film with a narrow strip of normal metal lying perpendicular to the direction of current flow.

Most of the experiments were done with structures using tin (Sn) as the superconductor and gold (Au) as the normal metal; however, a few structures of lead-copper (Pb-Cu) and indium alloy-copper (Indalloy-Cu) were also investigated. These combinations give $T_c' < T_c$ as required.

In the case of Pb-Cu structures, in addition to the narrow Cu underlay, the entire Pb film is overlayed with Cu while still under vacuum. This procedure has the dual purpose of protecting the exposed Pb from rapid oxidation, and of lowering the transition temperature of the lead by the proximity effect to temperature accessible in liquid helium.

It is known that lead and copper do not alloy at all (Hansen 1958); thus the depression of transition temperature in Pb-Cu is entirely due to the proximity effect (Smith et al 1961, Hilsch 1962, De Gennes 1964) a name given

to the phenomenon in which the superconductor is weakened by being in intimate contact with a normal metal.

Gold and tin form alloys and intermetallic compounds (Hansen 1958) which have transition temperatures lower than pure tin (Allen 1933). Chiou and Kolkholm (1964) and Kolkholm and Chiou (1966) attributed the depression of transition temperature of Sn films underlaid with Au or Ag to the presence of intermetallic compounds which they observed.

This indicates that in the case of Sn-Au NM structures the predominant effect responsible for depressing the transition temperature is alloying rather than the proximity effect.

The transition temperature of the weak section, T_c', was controlled by varying the relative thickness of the superconducting and normal metal films, and was set at temperatures between 2°K and 3°K for Sn-Au structures.

In the present work a thickness ratio of .25 (Au/Sn), gave a depression factor T_c'/T_c in the range .5 to .8, depending upon absolute thickness of the films and age of the structure. This compares reasonably with the results of Kolkholm and Chiou (1966) who find $T_c'/T_c \approx .5$ and Simmons and Douglass (1962) who find $T_c'/T_c \approx .7$ for films of Sn underlayed with Au and Ag, respectively, with a thickness ratio of.25 in both cases.

4-2 Fabrication.--For these experiments the following

fabrication procedure was found to be the most satisfactory, in that it could be carried out most easily with the available equipment and techniques.

A glass substrate was coated with collodion, which was then slit with a razor blade. The normal metal was evaporated through this slit and deposited onto the substrate. The sample was then removed from the evaporator to remove the collodion and excess metal by dissolving the collodion. The excess metal lying on top of the collodion had to be torn from the thin strip of metal deposited on the substrate. For this procedure to be successful, the metal had to adhere strongly to the substrate, which, when the metal was gold, presented a considerable problem in substrate preparation. This problem was solved by using a certain type of glass or by chemically cleaning and treating the glass surface.

After removal of the collodion and excess gold, four spots of indium were soldered to the corners of the substrate to form electrical contacts. The sample was then cleaned and replaced in the evaporator and a film of superconducting metal was deposited on top of the substrate, the strip of normal metal, and the indium contacts. The entire sample, including substrate, was about 1 cm^2 by about 1 to 2 mm thick.

The weak section was originally made several mm wide and later reduced to the desired width, w, by scratching

the metal films away with a needle, to produce the structure depicted in figure 4-1.

The metals were evaporated in a vacuum of 3×10^{-5} torr from a molybdenum boat heated by passing current through it. The thickness of the deposited film was determined by completely evaporating a known amount of metal in a fixed source-substrate geometry which had been previously calibrated by measuring the thickness of deposited films with an optical interferometer.

Due to the limitation of the evaporating technique and equipment the normal metal had to be exposed to air between the evaporations. It was found that when the normal metal was gold it could be exposed for days without imparing the operation of the completed superconducting structure. However, when the normal metal was copper, enough oxide formed in one day to render the completed structure inoperative.

Also, for this reason as well as others, the superconductor could not be deposited first. This indicates that the metals must be in intimate contact, since the oxide of tin under these conditions is less than 20Å thick (Kubaschewski and Hopkins 1962).

This structure has the important advantages that its geometry and dimensions are known and controllable, and its normal-state resistance and critical temperature are also

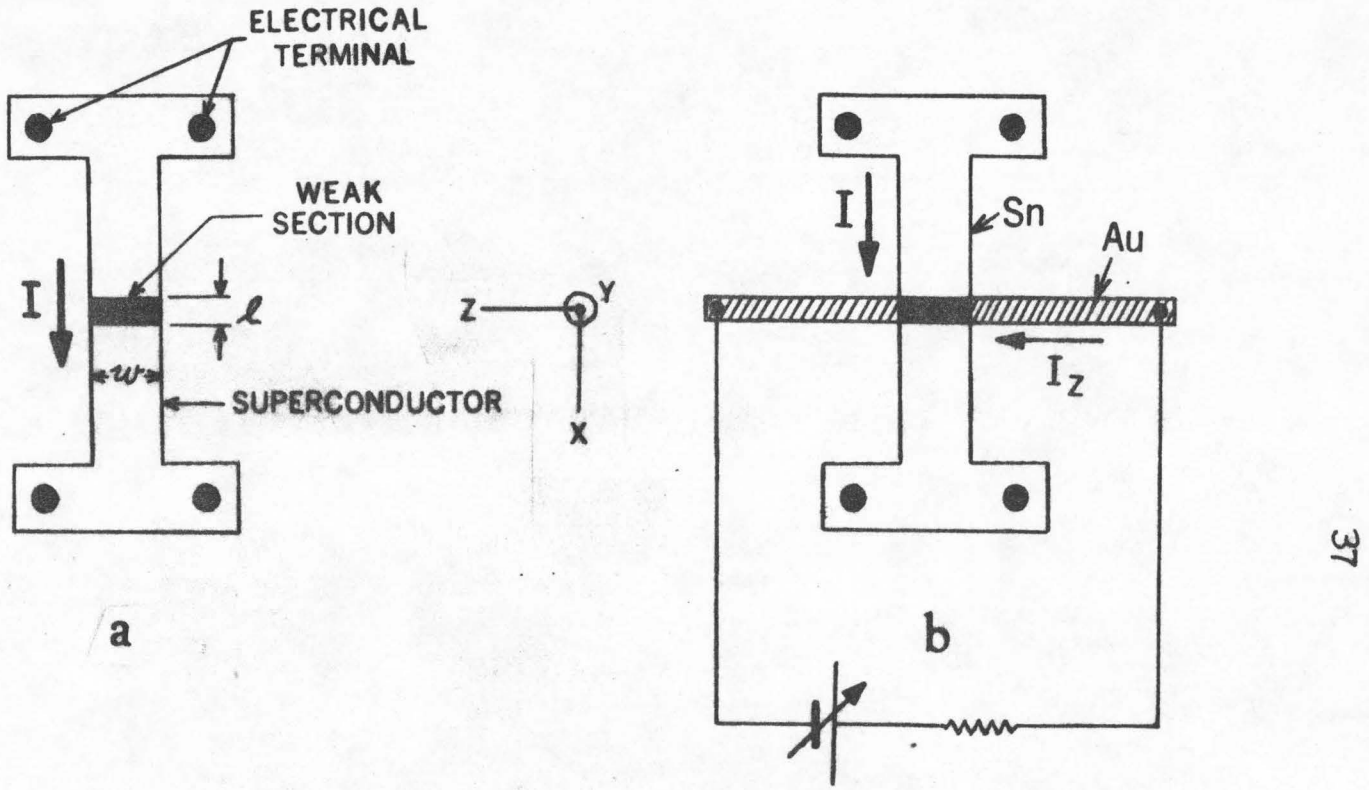

Fig. 4-1. (a) Geometry of NM weakly-superconducting thin-film structure; length, ℓ, and width, w, of weak section are shown, as well as direction of bias current, I. (b) Sn-Au NM structure with gold line extended, showing isolated current source and currents. Coordinate-axes used in text are also shown.

controllable.

The NM structure is convenient experimentally because it is relatively easy to make, its characteristics are stable and reproducible, and it is mechanically rugged. These structures were used repeatedly, when necessary, over a period of several months, the only precaution being to store them in a dessicator between uses.

There was some variation in sample parameters (for example, T_c') among different samples made under the same conditions, and variation in a single sample due to aging. However, it was found that in spite of such variations, the behavior of a particular sample was determined by the value of its parameters at the time of the experiment, and was independent of its history.

The Sn-Au structure was the only type studied enough to observe the effects of age. As a Sn-Au structure aged, its transition temperature T_c' increased, approaching T_c for the tin film, indicating a gradual dispersion of the gold into the tin.

4-3 Other Structures.--In regard to weak superconductivity, the NM structure is not unique: effects attributable to weak superconductivity have been observed in a variety of other structures. Among these are the Dayem bridge (Anderson and Dayem 1964): a thin film of superconductor with a restriction; structures consisting of a sandwich of super-

conductor-normal metal-superconductor (SNS) (Meissner 1958 and 1960, Clarke 1969, Bondarenko et al 1970); the point contact (Kanter and Vernon 1970a,b; Zimmerman and Silver 1964, 1966) made by pressing a superconducting point onto another superconductor; and the tin whisker or wire (Webb and Warburton 1968).

These other structures were not used in the present work because of various disadvantages associated with them. For example, the Dayem bridge does not have a geometrically well-defined weak section, its small size makes it difficult to fabricate, and its useful temperature range is small. The SNS structure has a large cross-sectional area which gives it a low resistance and makes measurement of its electrical characteristics difficult. The point contact does not have a well-defined geometry, and the nature of its structure is difficult to determine. In addition, it is unstable and fragile. The tin whisker is fragile and lengths of a few microns are difficult to obtain.

4-4 Size of Structures.--For these experiments, NM structures were fabricated to cover the following range of dimensions for the weak section: length, ℓ, $\lesssim 1\mu$ to 50μ; width, w, $\approx 5\mu$ to 2 mm; thickness, d, 300 Å to 3000 Å.

How do these dimensions compare with λ and ξ in the weak superconductor? Experimentally $\lambda(T = 0)$ is about 500 Å for Sn (Lock 1951). In the temperature range of these experiments, ρ is a fraction of its value at T = 0 and thus

$\lambda(T)$ is several times $\lambda(0)$. In addition, the term ξ_0/Λ contributes a factor of ≈ 5, so for these films λ is at least $\approx 1\,\mu$ (see section 2-11). The thin-film structures used here have a maximum thickness, d, of 3000 Å, thus $d/2 < \lambda$ and a magnetic field paralled to the film plane penetrates the film approximately uniformly. As will be shown later (section 6-1), ξ is at least $.3\mu$ for these structures.

The question now arises whether these structures satisfy the requirements of one-dimensionality as defined earlier. A criterion for one-dimensionality is that both w and d be approximately equal to or less than λ and ξ. It can be seen that d satisfies this requirement, but w is clearly much larger than either λ or ξ.

The requirement that w be less than λ and ξ may be relaxed if it is assumed that phase-slip will occur whenever the existence of a vortex is energetically unfavorable.

The energy per unit length, N, for a vortex line in a bulk superconductor is

$$N = \left(\frac{\varphi_0}{4\pi\lambda}\right)^2 \ln\frac{\lambda}{\xi} \qquad (4\text{-}1)$$

(De Gennes 1966). In a thin film ($d \ll \lambda$) the vortex is larger and requires more energy because the shielding currents are constrained to flow in the film and are less effective. (De Gennes 1966). The energy for a vortex in a thin film is

$$E = \left(\frac{\Phi_0}{4\pi\lambda}\right)^2 d \ln\frac{\lambda^2}{\xi d} \qquad (4\text{-}2)$$

Using the values for d, λ, and ξ given above gives an energy $E \approx 2 \times 10^{-19}$ joules. The energy available in the weak superconductor to form a vortex is $\frac{1}{2}L_K I_c^2$. Setting these two energies equal gives $I_c \approx 100\mu A$ as the minimum supercurrent necessary to allow the existence of a vortex.

In these experiments, structures were operated with I_c in the range $\sim 1\mu A$ to ~ 1 mA. Thus the samples were operated in both the regime where flux flow is forbidden and where it is possible. However, even in the regime where flux flow is possible according to the argument above, it still may not occur because it is energetically less favorable than phase-slip or is forbidden for other reasons.

The subject of flux flow will be considered again in sections 7-2 and 7-3 in connection with the experimental results.

In sections 2-5 and 2-6 it was stated that the vector potential could be neglected for these films. The justification for doing so is as follows (see Langer and Ambegaokar 1967).

Let the film lie in the xz-plane, centered in the y-direction, with the current j_s flowing in the x-direction. Since the thickness of the film d is small compared to the penetration depth, λ, the current will be distributed uni-

formly in the y-direction, and the resulting field inside the film will be

$$B_z \approx \mu y j_s/2 \tag{4-3}$$

Thus in the gauge used here

$$A_x = B_z y \approx \mu y^2 j_s/2 \tag{4-4}$$

Now compare j_s and the second term in equation (2-13) namely

$$\frac{2e\rho}{m} A_x \approx \frac{e\rho\mu}{m} y^2 j_s \approx (y/\lambda)^2 j_s \tag{4-5}$$

where equation (2-32) for λ was used. Thus since $y \leq d/2$ is small compared to λ the second term in equation (2-13) in the vector potential, $\vec{A}$, may be neglected.

In addition, this shows that in the case of a time varying supercurrent, in a film which is thin compared to λ, the magnetic inductance due to the $\vec{A}$ term is small compared to the kinetic inductance due to the $\nabla\theta$ term.

V. GENERAL EXPERIMENTAL TECHNIQUES

5-1 Temperature Control.--The superconducting structures used in these experiments were brought to low temperatures (1-4°K) by immersing them in a liquid-helium bath contained in a dewar, which was immersed in turn in a liquid-nitrogen bath contained in a larger second dewar.

The boiling temperature of liquid helium depends on its vapor pressure, and this fact allows a range of temperatures to be reached by pumping on the helium with a vacuum pump. For the apparatus used in these experiments, the approximate range was from 4.2°K at atmospheric pressure to 1.4°K at 2-3mm, the lower limit of the vacuum system. To maintain the temperature constant at a selected value, a mechanical pressure regulator was used.

Measuring the electrical characteristics of the superconducting structures involved voltages on the order of 10^{-7} to 10^{-8} volts, and sample impedances on the order of 10^{-1} to 10^{-3} ohms. Thus a reasonable amount of care was required in design and construction of the apparatus. The means taken to prevent invalidation of the data by interference are considered below.

5-2 Internal Interference.--At finite temperature there is noise in any system due to thermal fluctuations. In the case of electrical conductors it may be thought of as arising from the random fluctuations in occupancy of

states by electrons near the Fermi surface. At low frequencies ($h\omega \ll kT$), such as in these experiments, this noise is called Johnson noise.

Johnson noise is present in the superconducting structure itself when it is in a resistive state. Measuring the intrinsic noise of the superconductor was one part of the research and is discussed in section 7-2.

In order for measurements on the sample to be degraded, the apparatus connected to the sample would have to develop noise in the sample comparable to its intrinsic noise. To eliminate this possibility circuits which included the sample were kept at a high impedance relative to the sample. External circuit impedances were at least IKΩ at room temperature and at least 10Ω at liquid helium temperatures. Since the sample resistance was .1Ω or less, the external circuits may be considered as current sources.

Using the appropriate formula for Johnson noise:

$$\langle i^2 \rangle = \frac{4kT}{R} \qquad (5\text{-}1)$$

where i is the noise current in amps-hertz$^{-\frac{1}{2}}$ and R is the resistance of the noise source in ohms, it can be seen that the quietest sample (.1Ω at 4°) creates about 5×10^{-11} Amp-Hz$^{-\frac{1}{2}}$ of noise current whereas the external circuitry at worst creates only 5×10^{-12} Amp-Hz$^{-\frac{1}{2}}$ of noise current in the sample.

The total noise power in the sample can be estimated as follows. A typical inductance of a sample was on the order of 10^{-8} henry or greater; combined with a sample resistance of .1 Ω or less gives a maximum bandwidth of $\sim 10^{7}$ Hz. The total noise current from the sources considered above in a bandwidth of $\sim 10^{7}$ Hz would be about 2×10^{-8} amp, corresponding to a power of 4×10^{-17} watt induced in the sample. Thus the noise was insignificant compared to the signal that was being measured which had a power level on the order of 10^{-12} watt or greater, as will be shown later.

5-3 External Interference.--A number of precautions were taken in order to eliminate pickup of unwanted electromagnetic signals from outside sources. Sensitive electrical leads and apparatus were shielded and grounded. Electrical leads were kept short and leads connected to the sample from outside were provided with filters.

Any effects produced by interfering signals from broadcasting stations, electrical machinery, and the like, would be uncorrelated with experimental conditions and in addition would depend on the time of day, and the location of the apparatus. Such effects were looked for, but were not observed.

As an added precaution against unwanted signals or noise in the laboratory, many of the measurements were made

with all apparatus and the experimenter inside an electromagnetically shielded enclosure. The only electrical connection with the outside was the power mains, which were well filtered. It was found that the results were identical for experiments performed inside or outside of the shielded enclosure, confirming that adequate precautions had been taken originally in the design and construction of the apparatus.

5-4 Magnetic Shielding.--The experiment was sensitive to variations in the magnetic field, since the electrical characteristics of the superconducting structures which were being investigated depended strongly on the external magnetic field, as will be described in detail later.

To reduce interference from the ambient magnetic field, as well as electric fields, the dewars containing the sample were surrounded by two concentric, cylindrical mu-metal shields. Inside the shields the static magnetic field level was a few milligauss, and the time-varying component, principally at 60 Hz, was tens of microgauss.

The degree of sensitivity of a particular sample depended on its geometry. When experiments were done on the more sensitive samples, for which the tolerable field variation was a few milligauss, a lead shield was placed in the helium bath to further reduce field variations, and a coil placed near the sample was used to cancel any remaining

static field (the method used to set the field to zero will be described later). This coil was also used to apply a net field to the sample.

5-5 DC Measurements.--In order to measure the direct-current (DC) characteristics of the low-impedance sample a four-terminal connection was used as shown in figure 5-1. A direct measurement of the DC characteristic of the sample would have been difficult due to the low voltages involved, as well as the problems of currents generated by the thermocouple effect and drift. To avoid these difficulties the measurement was made using a "lock-in" (synchronous detection) technique with the reference frequency between 100 and 1000 Hz (but not at a multiple of 60 Hz to avoid interference from the power mains).

Two methods were used to measure the characteristics. In both cases the sample was biased by a DC current source connected to two of its terminals, and the other two terminals were connected to the input of the lock-in amplifier.

In the first method, the DC bias current, I, was chopped at the reference frequency, and the voltage pulses appearing across the sample were fed to the input of the lock-in amplifier, which measured the amplitude of the fundamental AC component of the pulses. Consequently, the output of the lock-in was proportional to the voltage, V, the sample would develop if a steady current I were passing

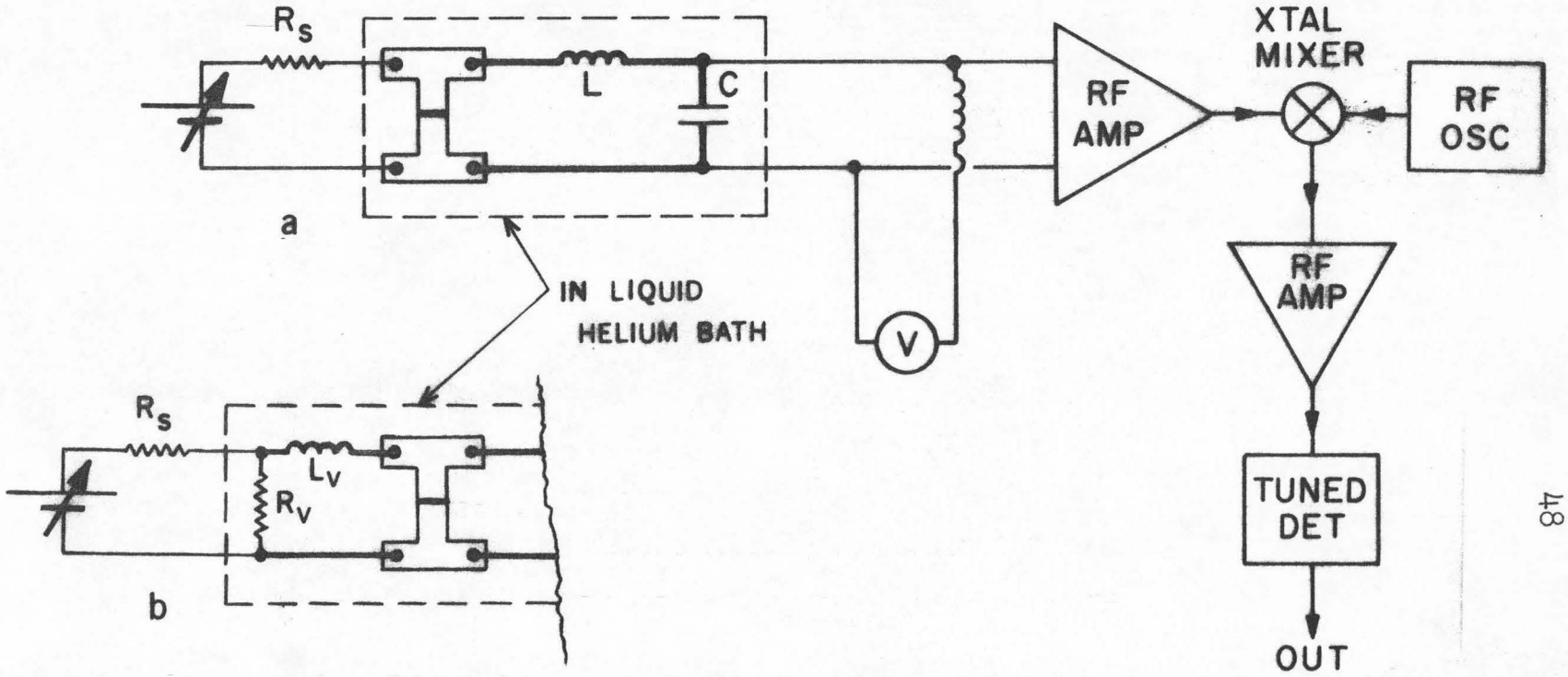

Fig. 5-1. Experimental arrangement used to measure electrical characteristics of samples. Heavy lines are superconducting. L,C form resonant circuit at 10 or 30 MHz. (a) using current biasing--R_S (IKΩ to 10MΩ) large compared to resistance of sample. (b) using voltage biasing--R_V ($\approx 6\mu\Omega$) small compared to resistance of sample. L_V is used to avoid loading the sample at high frequency.

through it. This repetitive measurement allowed the DC characteristic to be obtained using AC techniques, and would yield a V versus I curve as the DC bias current (I) was swept.

In the second method, a small AC current ($\sim 1 \mu A$) was added to the DC bias current; thus, the output of the lock-in amplifier was proportional to the dynamic resistance, dV/dI, of the characteristic curve at the bias point. This method yielded a dV/dI versus I curve as the DC bias current was swept.

To eliminate any DC currents that might flow due to thermocouple effects, capacitors were inserted in all possible current loops, with the exception of the circuit used to current bias the sample. The bias circuit consisted of a voltage source of several volts connected to the sample through a high resistance. For the level of accuracy in these experiments, the error introduced in the bias circuit by thermally generated voltages, on the order of millivolts, was insignificant.

5-6 RF Measurements.--Measurements were also made of the oscillating electric potential produced by the superconducting structures at the Josephson frequency, $\nu = V/\Phi_o$. This oscillationg potential was typically in the range of 10^{-8} to 10^{-7} volts, corresponding to a power level in the sample on the order of 10^{-12} watts. The oscillation was

detected at frequencies of approximately 10MHz and 30MHz.

In order to couple the low-impedance superconducting sample to an amplifier, the sample was made part of an LC resonant circuit which was also contained in the helium bath, as shown in figure 5-1. However, the impedance of the resonant circuit seen by the sample was not made so low that it loaded the sample significantly (loading was 10% at worst, and usually considerable less). The Q of the resonant circuit, and consequently its bandwidth and impedance, were varied, which produced the expected effects to be discussed later. The resonant circuit determined the bandwidth of the entire detection system which was typically .2 MHz at 30 MHz and .03 MHz at 10 MHz.

The resonant circuit was connected to a fixed-frequency detection system consisting of a superhetrodyne radio frequency (RF) amplifier and tuned detector. Thus the RF detection equipment was directly connected to the superconducting structure and did not rely on electromagnetic radiation for coupling. For purposes of determining the amplitude of the oscillation produced by the sample, the apparatus was calibrated with a RF signal of known amplitude applied at the input to the first amplifier.

The apparatus was designed so that the DC characteristics and high frequency oscillating potential could be measured concurrently.

5-7 Sensitivity.--The ultimate sensitivity of the measurements was limited by noise generated in the measuring apparatus. In the case of the DC measurements the noise was that generated in the input of the lock-in amplifier which was at room temperature, and allowed an ultimate sensitivity of a few nanovolts. In the case of the RF measurements the noise was that generated in the resonant circuit at liquid helium temperature which gave an ultimate sensitivity of about 10nV, which is the value expected for Johnson noise in the resonant circuit.

VI. DIRECT-CURRENT CHARACTERISTICS

6-1 Behavior Above T_c'.--Above T_c' all samples had a DC characteristic that gave a straight line on a V-I plot. The magnitude and temperature dependence of the resistance of the samples were as follows.

At room temperature (300° K) a measurement of the resistance of a sample represented mainly the resistance of the main film of superconductor, which was in the normal state, and gave a value of approximately 1 ohm per square for Sn-Au structures. This gives a resistivity of 10 x 10^{-6} ohm-cm which is in reasonable agreement with the accepted bulk value of 11.2 x 10^{-6} ohm-cm (NBS 1961).

As the temperature was lowered the resistance decreased, and at 4.2° it was less than the room temperature value by about a factor of twenty. The corresponding resistivity was .4 x 10^{-6} ohm-cm, which is 40 times the bulk value for pure tin at this temperature, which is 1.0 x 10^{-8} ohm-cm (NBS 1961). This descrepancy is due to contributions to the resistivity from impurities and the finite thickness of the film, both of which limit the mean free path of the conduction electrons.

Experimentally, it is found that the density of conductions electrons, n, is approximately 3 x 10^{22} cm^{-3} for tin, or about .8 conduction electron per atom (Sondheimer 1952), which gives a value of $\Lambda\rho \approx 1.4 \times 10^{-11}$ ohm-cm^2.

Thus the accepted resistivity for pure bulk tin gives $\Lambda \approx 1.4 \times 10^{-3}$ cm. For a film 1000 Å thick $d/\Lambda \approx 0.007$, and the expected ratio of film resistivity to bulk resistivity is 36 (Sondheimer 1952), in good agreement with the observed value of 40.

There is an abrupt drop in resistance when the main film becomes superconducting at its critical temperature T_c, which is about 3.8° K for Sn. The resistance remaining below T_c (but above T_c') is the normal-state resistance, R, of the weak section itself, and is determined by the composition and dimensions of the weak section. In these experiments the value of R ranged from about .5mΩ to .5Ω. For a weak section 1000 Å thick R is approximately .5Ω per square for Sn-Au and about 1Ω per square for Pb-Cu and In-Cu. This gives a resistivity of 5×10^{-6} ohm-cm and a mean free path of ≈300Å for the weak section in a Sn-Au structure, assuming that the material in the weak section has n approximately the same as n for tin. Thus, using formula (2-6) the coherence distance at absolute zero, $\xi(0)$, is $\approx 10^{-5}$ cm or 0.1μ.

The temperature dependence of ξ is

$$\xi(T) = \xi(0)(T_c/\Delta T)^{\frac{1}{2}} \qquad (6\text{-}1)$$

(De Gennes 1966). Thus for the temperature range of these experiments, $\Delta T/T_c \lesssim .1$, $\xi(T)$ is approximately .3μ or greater.

6-2 Behavior Below T_c'.--Below the critical temperature of the weak section, T_c', the V - I characteristic is no longer a straight line, but exhibits a zero-voltage supercurrent as shown in figures 6-1a and 7-1. The maximum value of this zero-voltage current is called the critical current, I_c.

6-3 Temperature Dependence of Critical Current.--I_c is temperature dependent, being 0 at T_c' by definition, and increasing with increasing $\Delta T \equiv T_c - T$. Over the temperature range in these experiments ($\Delta T/T_c' \lesssim .1$) the dependence of I_c on T was found to be approximately exponential.

However, comparing this dependence to any theory is difficult, because these experiments were designed with other purposes in mind and the experimental situation was far from ideal with respect to determining the dependence of I_c on T.

For these samples, the magnetic modulation period was less than 100 milligauss, thus I_c was sensitive to fields on the order of a few milligauss. Fields greater than this were produced by the current flowing in the sample for moderate critical currents. In addition, the large values of w/ℓ for the samples (30 and up) caused the field through the weak section of the sample to be distored and tended to make the samples even more sensitive to a magnetic field.

As a result of such complicating factors, the dependence of I_c on T seen here cannot be taken as characteristic

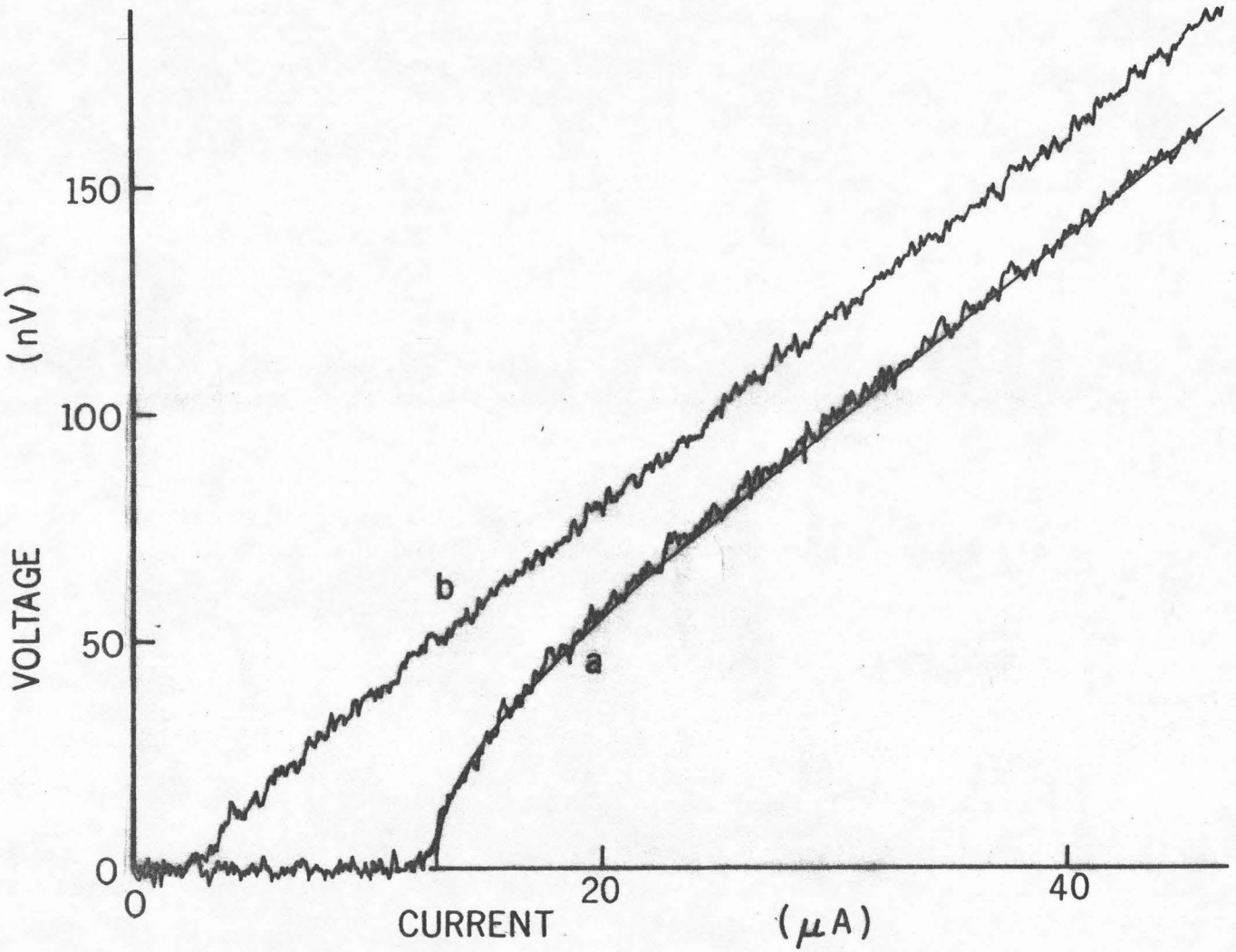

Fig. 6-1. V-I characteristic of NM-structure (a) without and (b) with applied B field.

of a weak superconductor. Determination of the dependence of I_c on T under more suitable conditions has been made by Notarys (1971), who found a ΔT^2 dependence for NM structures of the type used in the investigations described here. Dayem and Wiegand (1967) also find a ΔT^2 dependence of I_c for T close to T_c in the Dayem bridge (Anderson and Dayem 1964). A similar dependence has been observed by Meiklejohn (1964) in tin films which contained a few percent of indium. He ascribes the observed temperature dependence to the presence of the impurity (indium).

At present there is no theory to account for this dependence. The Ginsburg-Landon theory of superconductivity predicts a $\Delta T^{3/2}$ dependence for a pure homogeneous superconductor (Bardeen 1962).

6-4 Magnetic Field Dependence.--At any given temperature below T_c, I_c is a periodic function of the external applied magnetic field perpendicular to the plane of the film. As shown in figure 6-2, I_c is a maximum for B = 0 and has equally spaced minima and maxima as a function of B.

For an explanation of this effect, consider equation (2-13), integrated around the edge of the weak section. For such a closed path,

$$\oint \nabla\theta = 2\pi n \text{ and } \oint A = \phi. \qquad (6\text{-}2)$$

Thus if

$$\hbar 2\pi n \neq 2e\phi, \qquad (6\text{-}3)$$

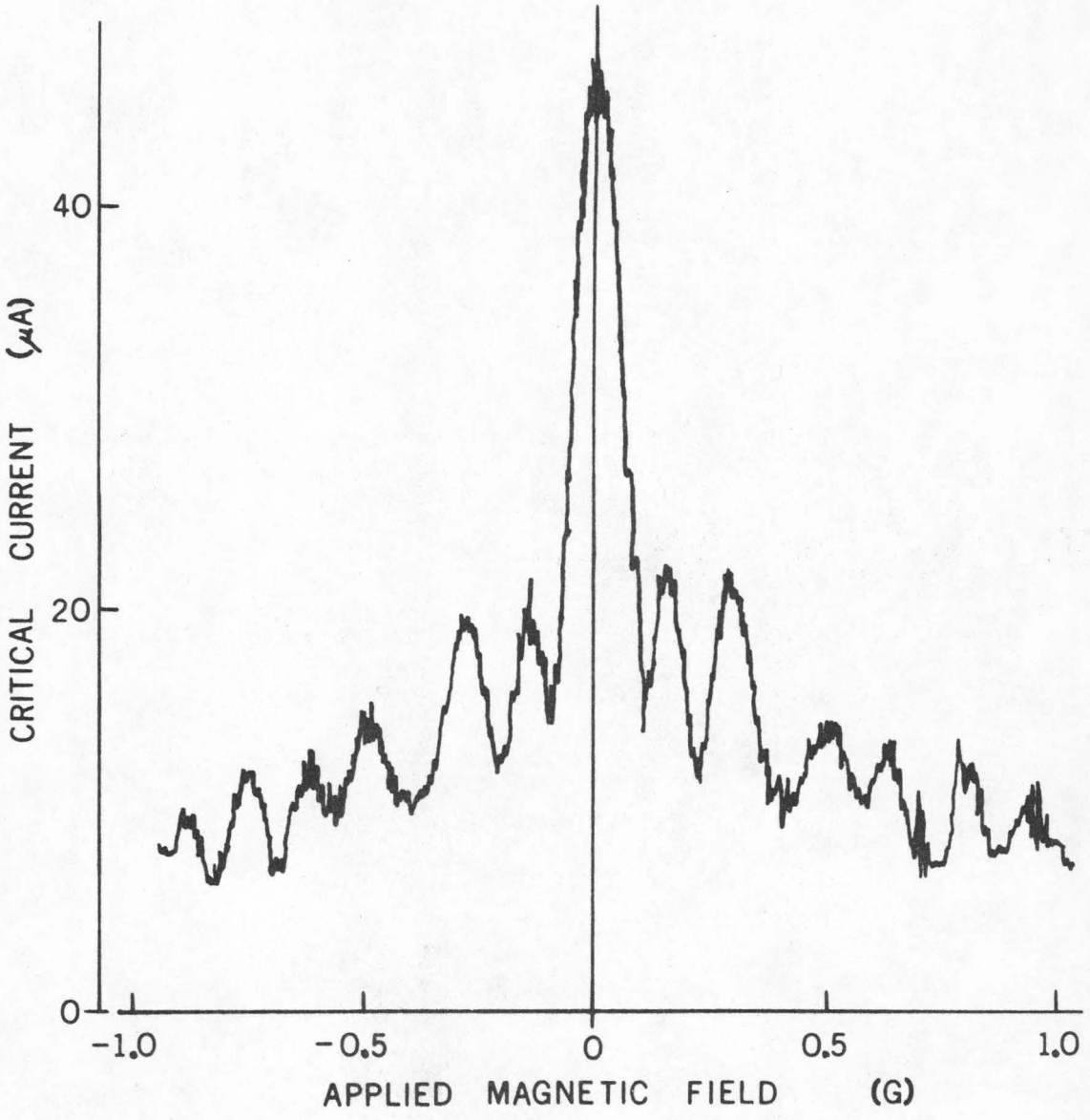

Fig. 6-2. Modulation of critical current of an NM weak superconductor by an external magnetic field. All minima and maxima are (approximately) equally spaced. Size of weak section is $\ell \approx 2\mu$, $w \approx 20\mu$, $d \approx 1000$ Å.

or

$$\Phi \neq n\frac{h}{2e} = n\,\Phi_o \qquad (6\text{-}4)$$

there would be a circulating current in the weak section. This circulating current would raise the energy of the superconductor and thereby decrease the critical current. Thus the critical current would be a periodic function of Φ, the flux in the weak section, and consequently of the applied field B, with period given by Φ_o/AREA (Parks and Little 1964). This effect is present in any superconductor, but only becomes important in a small superconductor, such as the NM structure.

Experimentally, it has been found that the period of the modulation is given by the flux quantum, Φ_o, divided by an effective area of the weak section. The effective area is larger than the actual area, ℓw, by a factor which depends on the ratio w/ℓ: for w/ℓ near 1, the factor is near 1, and for w/ℓ near 40 the factor is about 10. This effect is due to a distortion of the magnetic field by the superconductor which concentrates the field in the weak section (Notarys 1971).

The V-I characteristic, and magnetic modulation due to a small field perpendicular to the plane of the film, were found to be essentially the same when a Sn-Au weak superconductor was placed in a uniform, constant magnetic field of approximately 100 gauss parallel to the film (with-

in one degree) and perpendicular to the current in the weak superconductor.

Actually, the entire V-I characteristic is modulated by an external field--at finite voltage the current goes through minima and maxima as a function of field. This is illustrated in figure 6-1. Curves a and b were taken at the same temperature, curve a was taken with $B = 0$, I_c a maximum; curve b was taken for $B \neq 0$, with I_c at a minimum. However, it was found that for higher values of V and I, the interference became less well defined: the side peaks disappeared and the pattern was replaced by a single broad peak centered at $B = 0$. The effect is illustrated in figure 6-3 which shows the dependence of V on B for four values of the current, I. As I and V were increased the magnetic field pattern was seen to disappear when I was about three times I_c for I_c in the range of $10\mu A$ to $100\mu A$.

It has been suggested (Yu 1971) that the disappearance of the interference pattern is due to a time-varying magnetic field produced by the oscillating current in these structures, which tends to average out the fine structure of the pattern and leave only a broad peak.

6-5 Finite-Voltage Supercurrent.--The difference between V-I characteristics with and without an applied field, such as a and b in figure 6-1, is taken as a measure of the time-average supercurrent, $\langle I_s \rangle$, at any voltage V. It is assumed that any supercurrent has been suppressed, and that

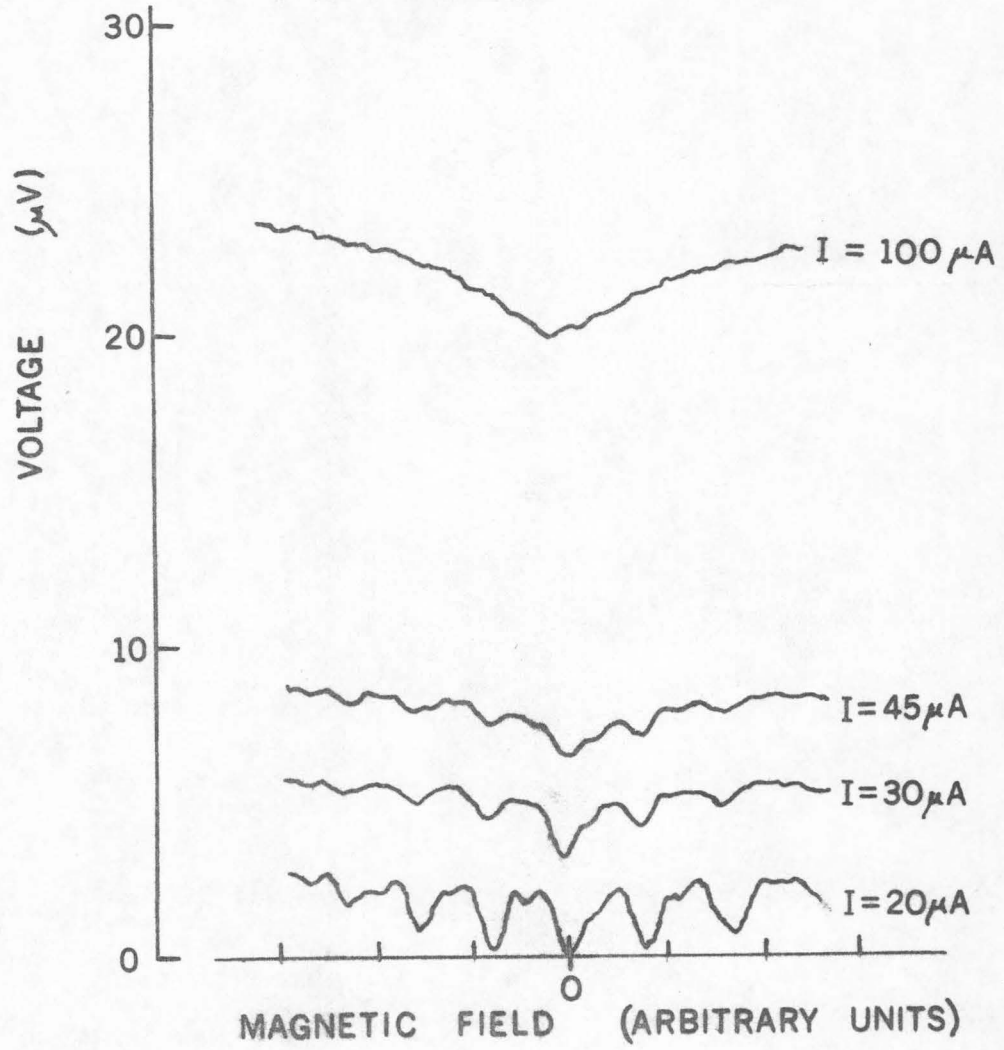

Fig. 6-3. Traces of voltage versus applied magnetic field with current, I, as a parameter, showing disappearance of magnetic modulation pattern as I increases.

curve b is the normal-state characteristic of the weak superconductor. The time-average supercurrent obtained in this way has been found to remain finite and constant out to at least .2mV for weak superconductors of Sn-Au.

For structures with short weak sections ($\ell \lesssim 4\mu$), and low critical current ($I_c \sim 10\mu A$), it was found that $\langle I_s \rangle$ was approximately $I_c/2$ for $\langle V \rangle \gtrsim I_c R$. In other words, for large I, $\langle V \rangle$ tended asymptotically to the value

$$\langle V \rangle = (I + I_c/2)R. \qquad (6\text{-}4)$$

On the basis of the two-fluid model presented in section 3-2 this result is consistent with repetitive phase slip between supercurrent states $I_s = I_c$ and $I_s = 0$. Using the two-fluid model, the weak superconductor may be simulated by a circuit consisting of a parallel combination of a resistor with value R, representing the normal current I_n and an inductor with value equal to the kinetic inductance, ℓ_K (section 2-10) representing the supercurrent I_s. For such a circuit, at high voltage ($\langle V \rangle \gtrsim I_c R$) the supercurrent increases from 0 to I_c uniformly in time and $\langle I_s \rangle \approx I_c/2$, whereas at low voltage ($\langle V \rangle \lesssim I_c R$) the supercurrent increases rapidly at first and then more slowly, and its time-average, $\langle I_s \rangle$, is closer to I_c. As can be seen from the experimental V-I characteristics (figures 6-1a and 7-1), this simple model is in good agreement with the observed behavior of the NM-structure.

Stewart (1968) and McCumber (1968) have developed a theory of a general Josephson junction which may be shunted by a resistance or capacitance. Their prediction is that in all cases for large I, $\langle V \rangle$ tends asymptotically to the value

$$\langle V \rangle = IR \qquad (6\text{-}5)$$

Hansma and co-workers (1971) have tested this theory with shunted Josephson junctions and find good agreement. Clarke (1971) finds that in SNS junctions at high voltage more current flows than predicted, which he attributes to vortex motion in the junction (sections 2-12 and 3-3). Thus the V-I characteristic of a weak superconductor cannot be explained on the basis of such a model of a Josephson junction.

For longer NM structures ($4\mu \lesssim \ell \lesssim 50\mu$) I_s was found to be more than $\approx I_c/2$, as would be expected for phase slip between two current states $I_s = I_c$ and $I_s = I_c - \Delta I_s > 0$ for phase slip by 2π, or between $I_s = I_c$ and $I_s = I_c - n\Delta I_s$ for phase slip by $2\pi n$. The exact value of $\langle I_s \rangle / I_c$ depends on the relative likelihood of phase-slips by 2π, 4π, $2\pi n$, ..., which is not known. However, the experimental results tended to indicate that a larger phase-slip is less likely.

VII. ALTERNATING-CURRENT CHARACTERISTICS

7-1 Oscillation.--The oscillating electric potential predicted by the phase-slip model in section 3-2 was observed at frequencies of 10 MHz and 34 MHz.

One method used to detect this oscillation was to current bias the weakly superconducting structure and observe the output of the fixed-frequency detection system described in section 5-6 (see figure 5-1a). When the bias current was swept, a detected signal would be observed when the voltage, $\langle V \rangle$, satisfied $\langle V \rangle = \nu_D \Phi_0$, where ν_D is the detection frequency, as shown in figure 7-1. The relation $\langle V \rangle = \nu_D \Phi_0$ was exact within the experimental accuracy of the voltage measurements, which was about 5%.

The oscillation was also detected when the superconducting sample was DC voltage-biased.(see figure 5-1b). The voltage source was placed in the helium bath and consisted of a resistor of about 6$\mu\Omega$ (a copper wire), which was connected across the sample with superconducting leads, one of which had an inductance of about 10^{-7} henry. Thus a sample with $R \approx 10$ mΩ was voltage biased only below about 10^4 Hz; this avoided loading the sample at the measuring frequency. Signals detected by this method are shown in figure 7-2.

Actually, regardless of the external circuitry, the sample is current biased for frequencies above a few tenths

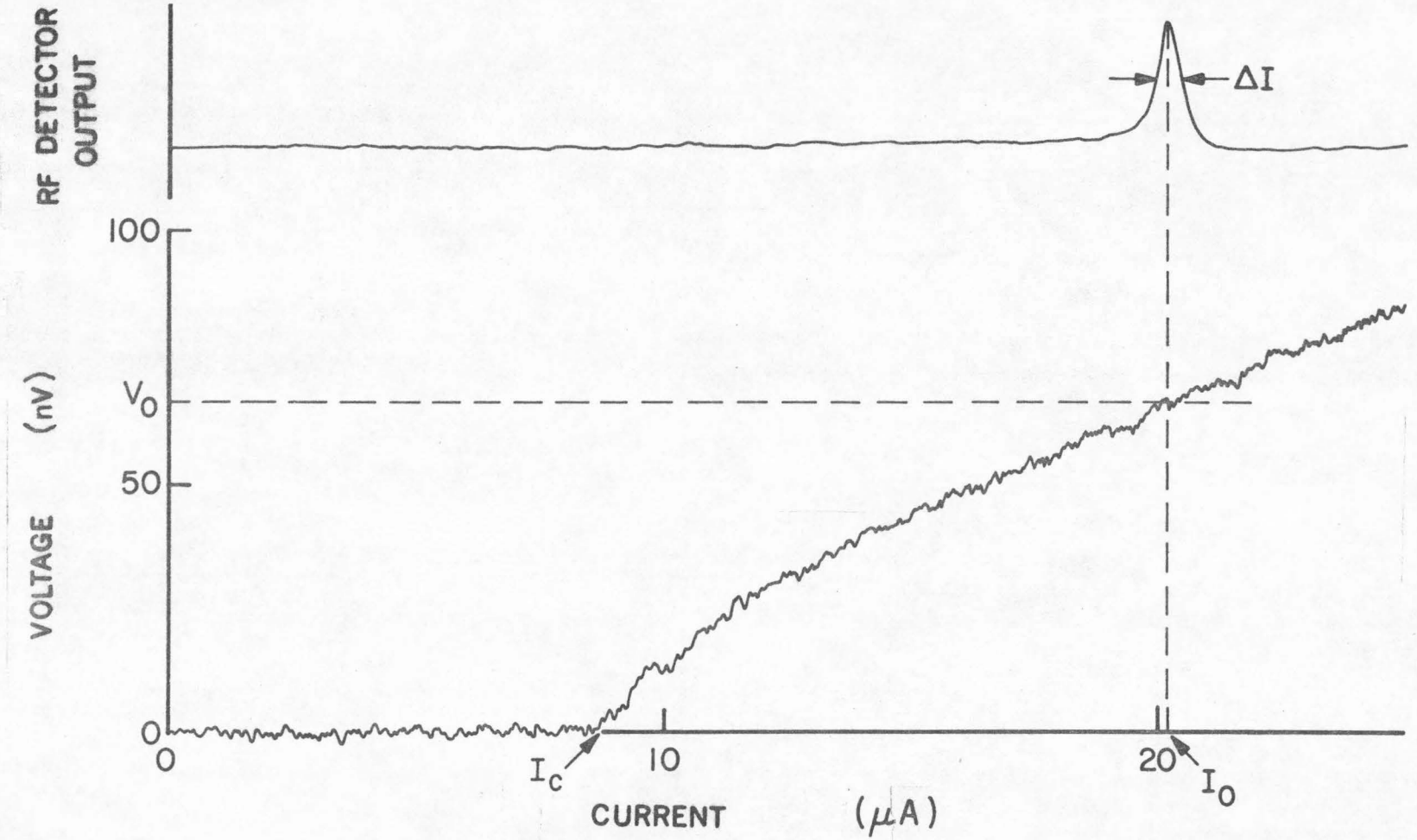

Fig. 7-1. V-I characteristic of NM structure showing detected signal when $\langle V \rangle = V_o = \nu_p \phi_o$ for $\nu_p \approx 34$ MHz.

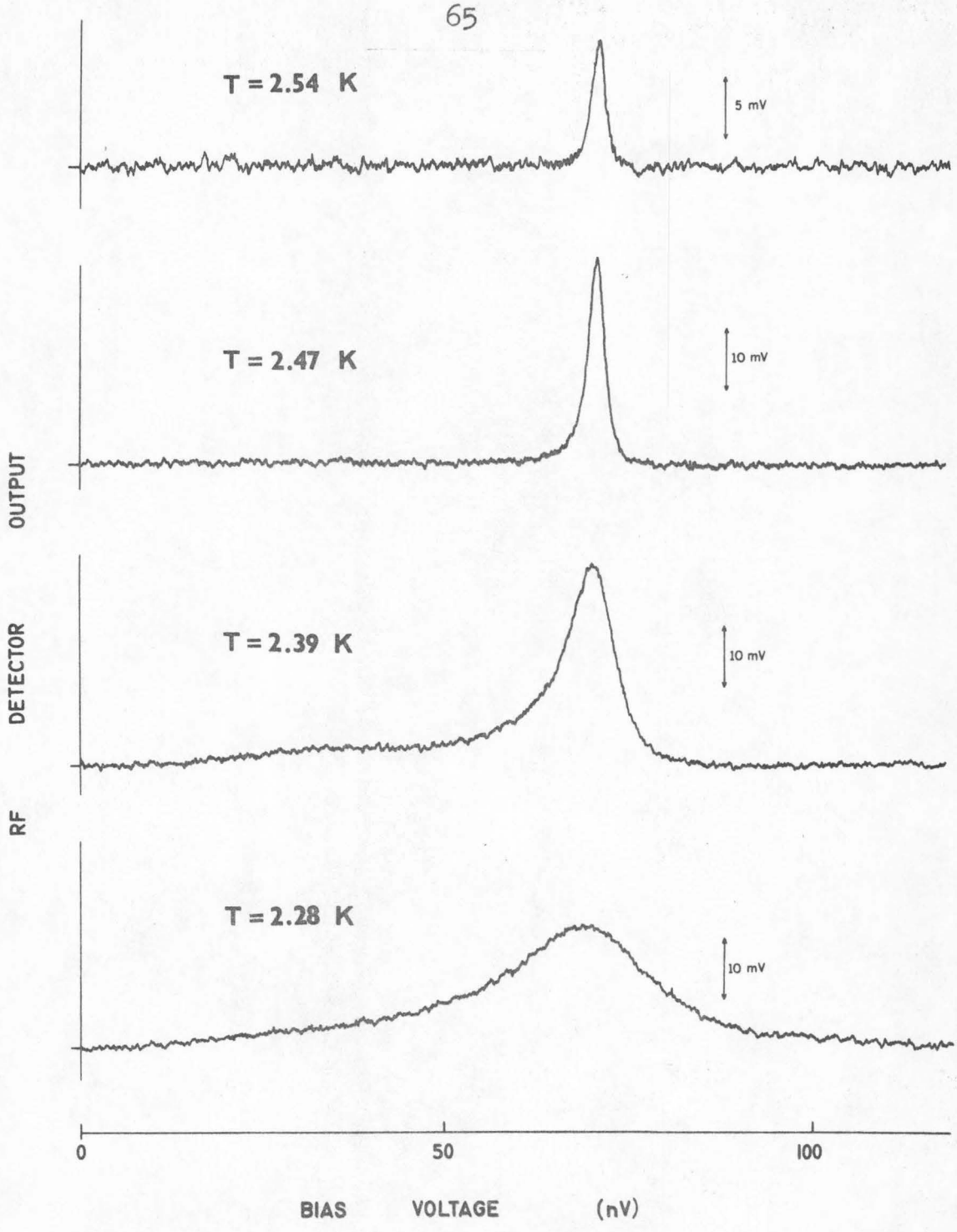

Fig. 7-2. Detected signal from voltage-biased NM structure at a frequency $\nu_D \approx 30$ MHz, as a function of temperature.

of a megahertz. This comes about because of the inductance of the main film on either side of the weak section, which has an inductance on the order of 10^{-8} henries.

7-2 Linewidth.--In either the voltage-biased or current-biased method of detection, the signal was observed to have a linewidth. When the linewidth of the signal was greater than the bandwidth of the detector, $\Delta\nu_D$, data such as figures 7-1 and 7-2 directly provided a value for the linewidth of the oscillation. The linewidths obtained by the two methods--current biasing or voltage biasing the sample--were the same within the experimental uncertainty.

A series of eleven samples was examined, covering the following range of parameters: ℓ = 2μ to 12μ, w = 60μ to 2 mm, d = 300 Å to 3000 Å. Normal state resistance, R, was .6 mΩ to 14 mΩ. Data for two typical samples are plotted in figure 7-3. Here the current linewidth, ΔI_s, obtained from current-biasing the sample, as in figure 7-1, is plotted against (TI_c).

For each of the eleven samples the slope of ΔI_s versus (TI_c) was .5 ± .1, and in magnitude all data fell within the limits set by the points in figure 7-3. Similar results were obtained for several samples of Pb-Cu and Indalloy-Cu.

Two procedures were performed to be certain that the observed linewidth was not a result of fluctuations in the critical current due to thermal fluctuations in the helium bath.

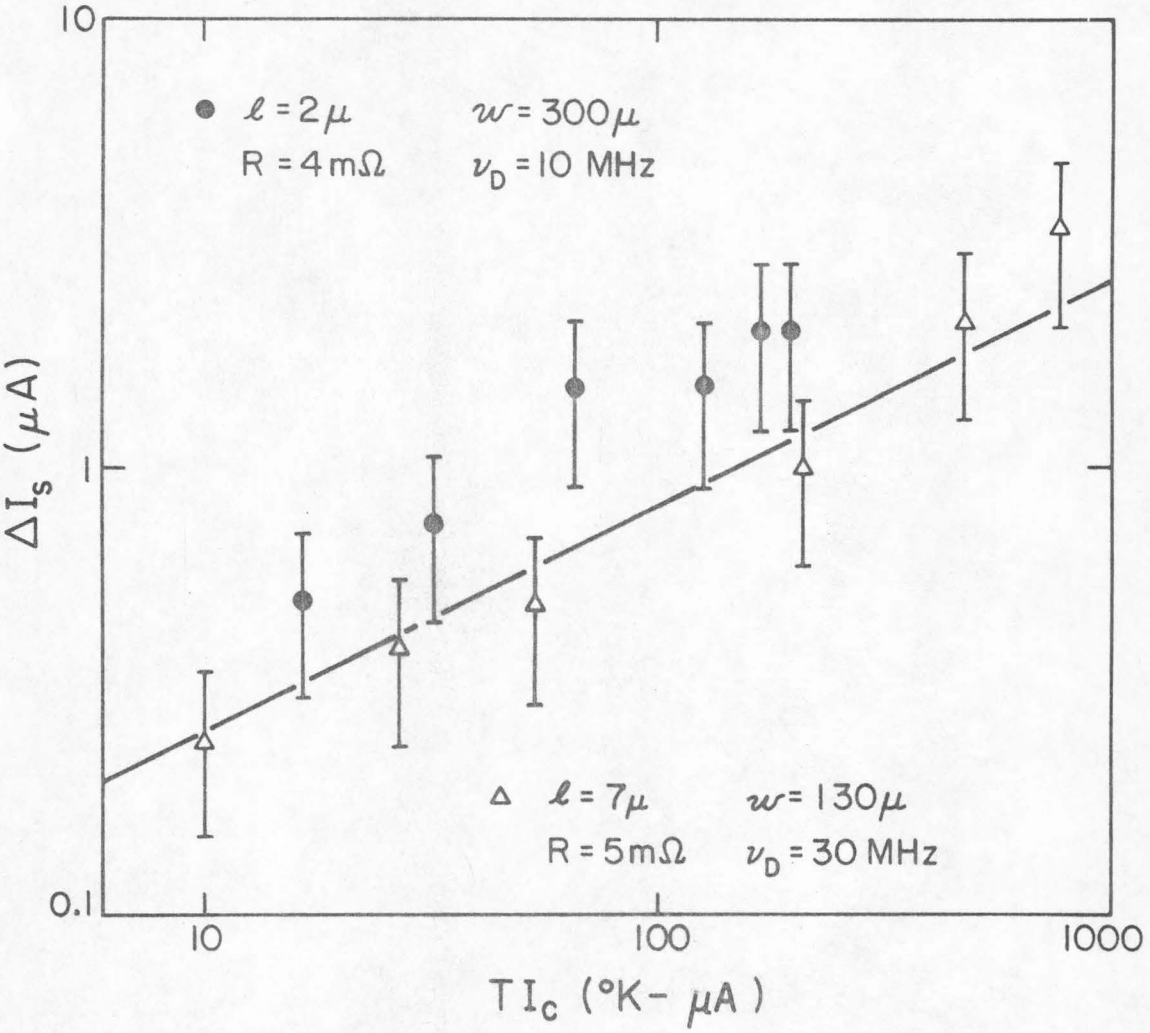

Fig. 7-3. Current noise, I_s, from two NM structures as a function of TI_c. Line is prediction based on Johnson noise.

The first procedure relied on the fact that helium becomes a superfluid below $T_\lambda = 2.18^\circ$ K, and its heat conductivity becomes extremely large (Leighton 1959). Because of this, thermal fluctuations in the bath are less below T_λ by at least an order of magnitude than they are above T_λ (Notarys 1971). There was no difference in the data for structures which operated above T_λ from those which operated below T_λ. In addition, a sample which had T_c' slightly above T_λ and operated both above and below T_λ showed no abrupt change in the linewidth on going throught T_λ.

The second procedure consisted in operating a sample alternately in the cold helium gas just above the liquid helium and in the liquid itself. Thermal fluctuations should be greatly different in the two cases. Again no difference in linewidth was observed.

It was also observed that the linewidth did not change when pumping of the helium vapor was interrupted, which reduces temperature fluctuations due to evaporation and boiling of the helium.

As a further check on the experiment, low frequency noise from as external source was fed to the sample and the signal was observed to widen, as expected. Its intensity decreased in a way such that the total power in the signal remained constant.

The linewidth data may be explained by use of the two-fluid model described in section 3-2. The normal current is assumed to have Johnson noise given by

$$\langle I_s^2 \rangle \approx \frac{kT}{R} \Delta\omega \qquad (7\text{-}1)$$

The appropriate bandwidth, $\Delta\omega$, is assumed to be given by the normal-state resistance, R, and kinetic inductance, $\mathcal{L}_K$, of the weak section: $\Delta\omega \approx R/\mathcal{L}_K$. This assumption is based on the fact that the sample is current biased, rather than voltage biased (see section 7-1) and that it has negligible capacitance. Consequently, it would be expected that the supercurrent must respond to Johnson noise in the normal current over the entire bandwidth, $\Delta\omega$. Thus

$$\langle I_s^2 \rangle \approx \frac{kT}{R}\left(\frac{R}{\mathcal{L}_K}\right) \approx \frac{kTI_c}{\Phi_o} \qquad (7\text{-}2)$$

where equation (2-30) for $L \approx 10\xi$ was used in the last step. An equivalent frequency linewidth, $\Delta\nu$, may be obtained by using the relations $dV/d\nu = \Phi_o$ and $dV/dI \approx R$. Thus

$$\Delta\nu^2 = \frac{kTI_cR^2}{\Phi_o^3} \qquad (7\text{-}3)$$

Equation (7-2) appears in figure 7-3 as a straight line and gives a reasonable good fit to the data. Thus the two-fluid model and the analysis given above appear to be a convenient way to interpret noise effects in the NM weakly-superconducting structure.

An analysis of noise appropriate to an insulating junction, such as the Josephson junction, has been made by Dahm and co-workers (1969). The functional dependence of the linewidth on the parameters T, I, V, etc. predicted by this analysis does not agree with that observed for the NM weakly superconducting structures. In addition, for large values of the current, the observed linewidth is smaller by a factor of 4 than that predicted on the basis of the theory of Dahm and co-workers.

7-3 Amplitude.--The absolute amplitude of the oscillating potential was obtained by multiplying the intensity of the detected signal by its linewidth. Reduced data from three samples are shown in figure 7-4.

It can be seen that for $\langle V \rangle \gtrsim I_c R$ the RMS AC potential, v, obeys

$$v \approx I_c R / 2^{3/2} \qquad (7\text{-}4)$$

in agreement with the result expected (equation 3-1) for the model of weak superconductivity presented in section (3-2). As pointed out in section 4-4, for large I_c there is a possibility of flux flow in these structures. For flux flow

$$v \approx \sqrt{2} \langle V \rangle \qquad (3\text{-}2)$$

with which the data for large I_c are in agreement, whether or not flux flow is actually occurring.

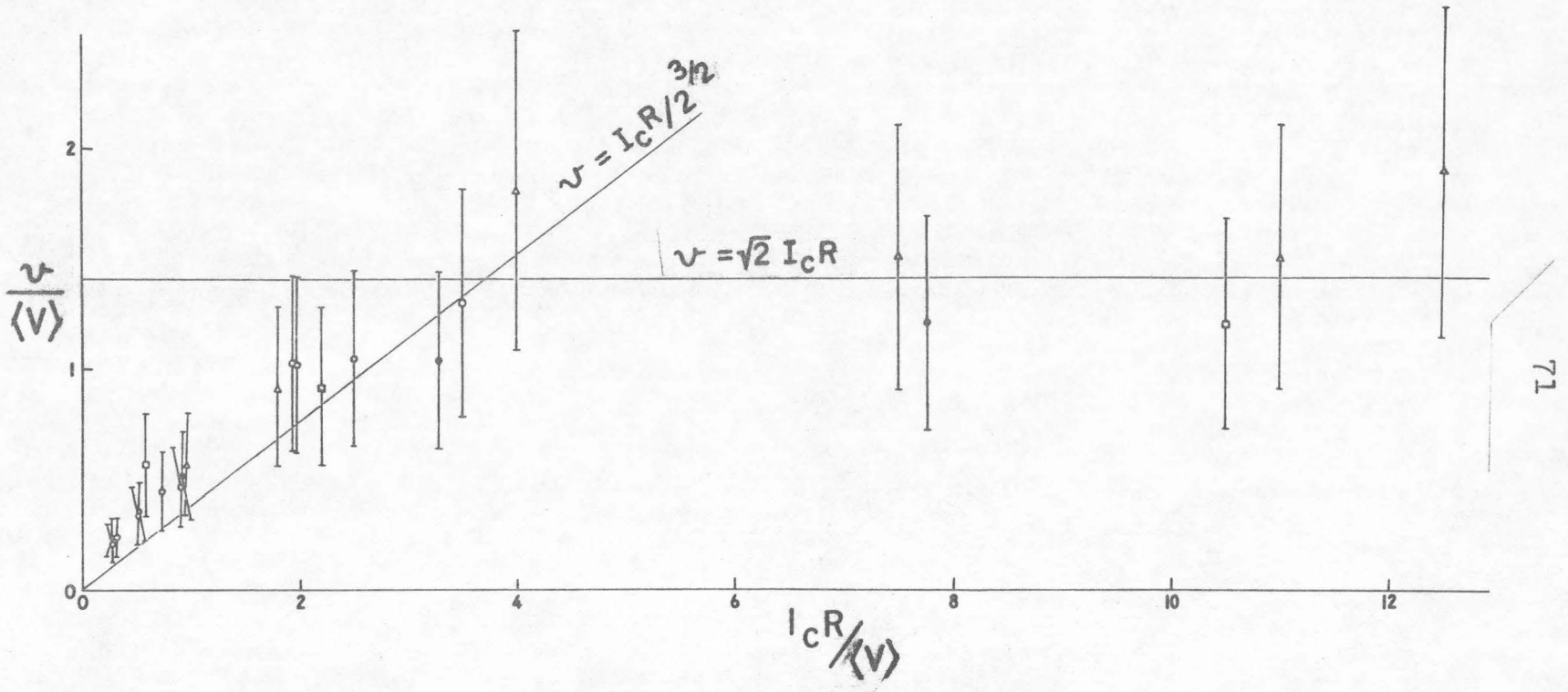

Fig. 7-4. Amplitude of oscillating potential, v, produced by NM structures. All samples Sn-Au, d $\approx$ 1000 Å, $\ell \approx 2\mu$. Δ w = 300μ, R$\approx$4mΩ, $\nu \approx$ 10MHz O, $\bullet$ w = 200μ, R$\approx$4mΩ, $\nu \approx$ 30MHz $\square$ w = 1000μ, R$\approx$2mΩ, $\nu \approx$ 10 MHz

7-4 Effects of Magnetic Field.--For most of the measurements of linewidth and amplitude the external magnetic field was adjusted as nearly as possible to give the maximum I_c. From knowledge of the modulation it was assumed that for maximum I_c the net applied field was zero and that any small residual field had been cancelled.

A question naturally arises as to the possible effects on the data of a non-zero net applied magnetic field. To answer this question, a number of experiments were performed in which the magnetic field was varied over many modulation periods and data on linewidth and amplitude were taken as before. When B was varied, the observed linewidth and amplitude were observed to change, as did the critical current. However, the observed linewidth and amplitude had the same dependence on I_c as for B = 0. In other words, the linewidth and amplitude are determined by T, R, and I_c, regardless of the applied field B (even though I_c depended on B).

7-5 Empirical Summary.--For structures with ℓ short, less than about 4μ, the experimental results for the DC and AC characteristics are summarized in the following empirical formula

$$I_s(t) = \frac{I_c(B)}{2}\left[1 + \cos 2e/\hbar \int_0^t V(t')dt'\right] \qquad (7\text{-}5)$$

If the structure is current biased--which is almost always the case--then in addition

$$V(t) = (I-I_s)R \qquad (7\text{-}6)$$

This formula for the supercurrent is similar to that for the Josephson junction, equation (2-35), but includes an additional term to reflect the excess supercurrent and the dissipative nature of weak superconductivity discussed in section 3-2.

The solution of equations (7-5) and (7-6) is

$$V(t) = \frac{2I/I_c(1-I/I_c)\epsilon}{1 + \epsilon \sin\omega t} \qquad (7\text{-}7)$$

which yields

$$\langle V(t)\rangle = \sqrt{I(I-I_c)}R \qquad (7\text{-}8)$$

and

$$v(t)/\langle V(t)\rangle = \sqrt{2}\,(\sqrt{1-\epsilon^2}\,-1)/\epsilon \qquad (7\text{-}9)$$

where

$$\omega \equiv \frac{2\pi\langle V(t)\rangle}{\Phi_o}\,, \qquad \epsilon \equiv (1-2I/I_c)^{-1} \qquad (7\text{-}10)$$

The DC characteristic given by equation (7-8) is plotted in figure 6-1a using only the measured values of R and I_c, and is seen to agree well with the measured V-I curve.

From equation (7-7) it can be seen that for $I \gg I_c$ $v \approx \frac{1}{2\sqrt{2}} I_c R$ and V(t) has a small harmonic component and a DC component. For $I \approx I_c (\epsilon \approx -1)$, V(t) is strongly anharmonic --pulse-like--and $v \approx \sqrt{2}\langle V\rangle$, as would be expected for flux flow (section 3-3). These results are plotted on figure 7-4. In both regions there is good agreement with the data.

7-6 Effect of Resonant Circuit.--It was hypothesized that when the high Q LC resonant circuit was connected to the sample there might be a distortion in the DC V-I curve near $V = \phi_0 \nu_D$ due to loading of the sample by the resonant circuit or due to a tendency of the sample to oscillate at the frequency of the resonant circuit over an extended range of bias current, I. At present there is no theoretical basis for acceptance or rejection of such an hypothesis.

Such an effect was carefully looked for experimentally but was not observed. The absence of an observed effect could be due to the hypothesis being false, or due to the coupling of the sample to the resonant circuit being so slight that the effect was unnoticeable.

It was observed that when the current through the sample was greater than I_c, the background noise level in the RF detection system was lower than when the current was less than I_c. This effect was due to a change in Q of the resonant circuit due to the appearance of the normal state resistance of the bridge above I_c. The direction and magnitude of the effect were found to be compatible with such an interpretation. When a low Q resonant circuit was used, the effect disappeared.

An experiment was also done to see if the structure could be loaded by coupling it to an external spin system to produce a distortion in the DC V-I characteristic.

In this experiment a substance known as DPPH (diphenye picryl hydrazyl) (Holden et al 1950, Townes and Turkevich 1950, Hutchison, et al 1952) in the form of a powder was placed directly on top of the weak section of an NM structure. DPPH exhibits a strong, sharp paramagnetic spin resonance in a magnetic field at approximately 2.8 MHz/gauss. The experiment was done in a magnetic field which was varied from 50 - 200 gauss, parallel to the plane of the film and both parallel and perpendicular to the current in the superconductor. This arrangement was calculated to load the NM weakly superconducting structure significantly assuming a coupling between the spin system and the weak superconductor of 10^{-4} or greater.

No effect attributable to the presence of the DPPH was observed in the V-I characteristic despite repeated attempts. As in the case mentioned at the beginning of this section, this may be due to insufficient coupling, or due to the fact that loading the weak superconductor does not cause a distortion in the V-I characteristic which would also explain the observation reported at the beginning of this section.

7-7 Harmonics.--In addition to the main signal at a sample voltage $V = \nu_D \Phi_o$, a signal was occasionally observed when the sample voltage was one-half this value, at $\nu_D = 2V/\Phi_o$ (see figure 7-5). This signal is due to harmonic generation by the sample. Such signals were observed only when

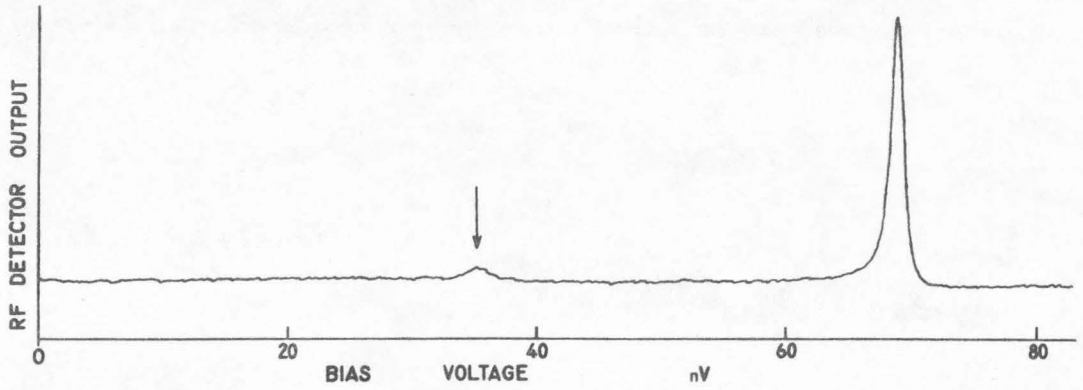

Fig. 7-5. Detected oscillation from voltage-biased NM structure showing harmonic generation (arrow).

$I_cR \gtrsim \langle V \rangle$, which would tend to support the hypothesis that the oscillation deviates markedly from a sinewave for $I_cR \gtrsim \langle V \rangle$. The harmonic signals were always weak which makes an accurate estimate of their amplitude impossible.

Only the signal corresponding to the second harmonic was identified. Whether higher harmonics were present is not known as it is likely that they were too weak to be detected. It is also possible that signals such as that in figure 7-2 indicate the presence of a harmonic, or harmonics, which blend into the main signal on the low voltage side.

7-8 Phase Slip by Multiples of 2π.--In section 2-8 it was argued that in structures with a long weak section $L \gg 10\xi$ there could be phase slip by 4π, 6π, ... If such were the case there would be an oscillation for which $V = n\nu\Phi_0$ since the reduction in phase which occurs during phase slip need occur only a fraction as often when each reduction in phase is greater.

A signal satisfying $\langle V \rangle = 2\nu\Phi_0$ was observed in a Sn-Au structure with $l \approx 14\mu$, in addition to the usual signal at $\langle V \rangle = \nu\Phi_0$. This would tend to indicate that the coherence distance in the weak section at the temperature of the experiment (for which $\Delta T/T_c \approx .02$) was on the order of $.7\mu$, giving $\xi(0) \approx .15\mu$. This is in good agreement with the value predicted from the experimental DC characteristics in sections 6-1 and 6-5, assuming that the effective length, L, of

the weak section is approximately equal to its geometric length, ℓ, for these structures.

7-9 External Radiation.--If external radiation of frequency ω is applied to these structures, constant-voltage "steps" can be made to appear in the DC V-I characteristic, as shown in figure 7-6, at voltages given by $V = n \frac{\hbar}{2e}\omega$, n an integer.

In a similar manner, steps can also be made to appear in the DC characteristic of a Josephson junction by application of external radiation. In the case of the Josephson junction, an analysis is possible because the basic equations are known (see section 2-13). In the case of a junction that is voltage biased at DC, the equations are

$$\dot{\theta}(t') = \frac{2e}{\hbar}(V_o + V_1 \cos\omega_1 t'), \qquad (7\text{-}11)$$

where V_o is the DC voltage and $V_1\cos\omega_1 t'$ is the applied signal; and

$$I_s(t) = I_o \sin \int_o^t \theta(t')dt' \qquad (7\text{-}12)$$

where I_o is a current that depends on the junction and conditions of the experiment. Thus

$$I_s(t) = I_o \sin\left\{\frac{2e}{\hbar}\int_o^t (V_o + V_1\cos\omega_1 t')dt'\right\} \qquad (7\text{-}13)$$

which yields

$$I_s(t) = I_o \sin\left\{\frac{2e}{\hbar} V_o t + \frac{2eV_1 \sin\omega_1 t}{\hbar\omega_1} + \alpha\right\} \qquad (7\text{-}14)$$

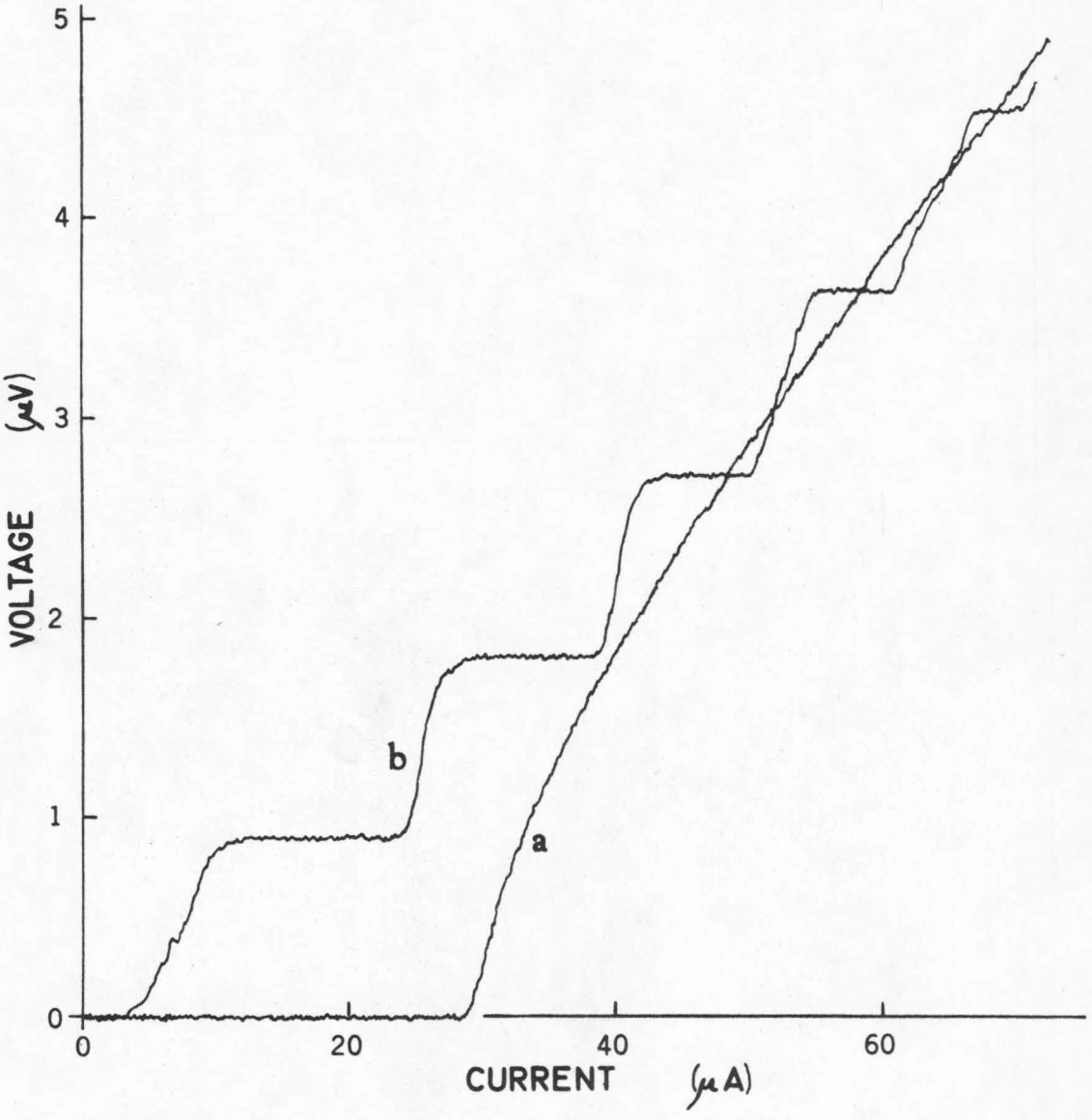

Fig. 7-6. Voltage-current characteristic of NM structure, showing constant-voltage "steps" produced by external radiation (a) No external radiation (b) external radiation at approximately 500 MHz applied.

where α is a constant of integration.

The right-hand side may be expanded in terms of bessel functions to give

$$I_s(t) = I_o \sum_{n=-\infty}^{\infty} \left\{ J_n\left(\frac{2eV_1}{\hbar\omega_1}\right) \sin\left[\left(n\omega_1 + \frac{2eV_o}{\hbar}\right)t + \alpha\right]\right\} \quad (7\text{-}15)$$

to determine the resultant DC characteristic, I_s (t) must be averaged with respect to time. Due to the sine term all terms average to zero except when the sine is a constant, that is, when

$$n\omega_1 = -\frac{2eV_o}{\hbar}, \quad (7\text{-}16)$$

as expected. When this equation is satisfied, $\langle I_s(t)\rangle \neq 0$, and there is a constant voltage step. These steps may be thought of as the DC component resulting when the internal and external oscillations, or their harmonics, mix.

A similar result will be obtained if the empirical equation (7-5) for weak superconductivity is used in place of equation (7-12), although the exact nature of the solution will be different.

The noise which gives rise to the broadening of the oscillation in the NM structure should also affect the observed steps. This is supported by experimental evidence: it was found that steps could not be produced for external radiation below a frequency on the order of $\Delta\nu$, the linewidth given by equation 7-3. For these experiments $\Delta\nu$ ranged from ~1 MHz to ~100 MHz.

In addition, the rounding at the edges of steps is in qualitative agreement with that expected from noise according to the analysis in section 7-2.

Another effect of external radiation on these NM structures is that, for frequencies in the microwave region ($\sim$10 GHz), the critical current, I_c, initially increases as the applied microwave power is increased from zero (Notarys and Mercereau 1969).

Such an effect was also observed by Dayem and Wiegand (1967) and Anderson and Dayem (1964) for their constricted thin film structures. So far, no explanation for this phenomenon is known. It has been looked for in the Josephson junction but has not been observed (Dayem and Wiegand 1967).

7-10 Radiation by NM Structures.--Since there is an oscillation in these weakly superconducting structures, and since they couple to external radiation, it is clear that they radiate some electromagnetic energy. However, their low impedance, on the order of .1Ω or less prevents them from coupling well to free space or ordinary antennas and would lead one to believe that the power radiated would be a very small fraction of the total RF power available.

A confirmation of this fact was made by a calorimetric measurement which showed that within the experimental accuracy of 10%, all the electrical input power to one of

these structures was converted to heat in the structure itself. A sample with $R \approx .1\Omega$ was used and I_c ranged from approximately 10μA to 1 mA. Input powers less than 10^{-9} watt were measured. Of the total input power, the portion associated with the oscillation ranged from a few percent to about fifty percent depending on the experimental conditions.

7-11 Crossed Currents.--Two Sn-Au NM structures were made with the gold strip extended on either side of the weak section as shown in figure 4-1b. The two gold strips were connected to an isolated current source to study the effect of a current, I_z, in the weak section perpendicular to the bias current. DC and AC measurements were made in the same manner as before using current biasing.

The only effect was a displacement of the V-I characteristic along the I-axis by an amount equal to a fraction of the crosswise current I_x. The fraction was different for the two structures and was about $\frac{1}{2}$.

This algebraic addition of currents can be explained by assuming that the current I_z does not flow across the weak section perpendicular to the bias current, I, as originally intended. Instead, due to some asymmetry where the gold strip joins the structure the current I_z flows into the tin first and then across the weak section parallel to the bias current. For these structures w was 200μ; ℓ, 2μ and d, 1000 Å. Obviously this geometry is not suitable for doing

the experiment originally intended.

VIII. REFERENCES

ALLEN, J. F. 1933 Phil. Mag. 16, 1005.

ANDERSON, P. W. 1966, Rev. Mod. Phys. 38, 298.

ANDERSON, P. W. and A. H. Dayem 1964, Phys. Rev Letters 13, 195.

BARDEEN, john 1962, Rev. Mod. Phys. 34, 667.

BARDEEN, J., L. N. Cooper and J. R. Schrieffer 1957a, Phys. Rev. 106, 162.

BARDEEN, J., L. N. Cooper and J. R. Schrieffer 1957b, Phys. Rev. 108, 1175.

BONDARENKO, S. I., I. M. Dmitrenko and E. I. Balanov 1970, Soviet Physics--Solid State 12, 1113 (translated from Fizika Tverdogo Tela 12, 1417 (1970)).

BYERS, N. and C. N. Yang 1961, Phys. Rev. Letters 7, 46.

CLARKE, J. 1969, Proc. Roy. Soc. (London) A308, 447.

CLARKE, John 1970, Am. J. Phys. 38, 1071.

CLARKE, John 1971, preprint UCRL-20548, University of California, Lawrence Radiation Laboratory, Berkeley, California.

CHIOU, C. and Kolkholm, E. 1964, Acta Met. 12, 883.

DAHM, A. J., A Denenstein, D. N. Langenberg, W. H. Parker Parker, D. Rogovin and D. J. Scalapino 1969 Phys. Rev. Letters 22, 1416.

DAYEM, A. H. and J. J. Wiegand 1967, Phys. Rev. 155, 419.

De GENNES, P. G. 1964, Rev. Mod. Phys. 36, 225.

De GENNES, P. G. 1966, Superconductivity of Metals and Alloys, W. A. Benjamin, Inc. (New York).

EISBERG, Robert Martin 1961, Fundamentals of Modern Physics, John Wiley and Sons (New York) chapter 7.

FEYNMAN, Richard P., Robert B. Leighton and Matthew Sands 1965, The Feynman Lectures on Physics, vol. III, Addison-Wesley Publishing Co. (Reading, Massachusetts) chapter 21.

FILE, J. and R. G. Mills. 1963, Phys. Rev. Letters 10, 93.

FRIEBERTSHAUSER, P. E., H. A. Notarys and J. E. Mercereau 1968, Bull. Am. Phys. Soc. 13, 1670.

HANSEN, Max 1958, Constitution of Binary Alloys, (second edition) McGraw-Hill (New York).

HANSMA, P. K., J. N. Sweet and G. I. Rochlin 1971, preprint UCRL-20590, University of California, Lawrence Radiation Laboratory, Berkeley, California.

HILSCH, Peter 1962, Z. Physik 167, 511.

HOLDEN, A. N., C. Kittel, F. R. Merritt and W. A. Yager 1950, Phys. Rev. 77, 147.

HUTCHISON, Clyde A. Jr., Ricardo C. Pastor and Arthur Kowalsky 1952, J. Chem. Phys. 20, 534.

JACKSON, John David 1962, Classical Electrodynamics, John Wiley and Sons, Inc. (New York) p. 140.

JOSEPHSON, B. D. 1962 Phys. Letters 1, 251.

KANTER, H. and F. L. Vernon, Jr. 1970a, Appl. Phys. Letters 16, 115.

KANTER, H. and F. L. Vernon, Jr. 1970b, Phys. Rev. Letters 16, 588.

KIM, Y. B., C. F. Hempstead and A. R. Strnad 1965, Phys. Rev. 139, A1163.

KIRSCHMAN, R. K., and J. E. Mercereau 1971, Phys. Letters 35A, 177.

KIRSCHMAN, R. K., H. A. Notarys and J. E. Mercereau 1971, 34A, 209.

KITTEL, Charles 1971, Introduction to Solid State Physics, (fourth edition) John Wiley and Sons, Inc. (new York) chapters 7 and 12, advanced topics J and M.

KOLKHOLM, E. and C. Chiou 1966, Acta Met. 14, 565.

KUBASCHEWSKI, O. and B. E. Hopkins 1962, Oxidation of Metals and Alloys, (second edition) Academic Press, Inc. (London) p. 38.

LANGER, J. S. and Vinay Ambegaokar 1967, Phys. Rev. 164, 498.

LEIGHTON, Robert B. 1959, Principles of Modern Physics, McGraw-Hill Book Company, Inc. (New York) pp. 368-369.

LITTLE, W. A. 1967, Phys. Rev. 156, 396.

LOCK, J. M. 1951, Proc. Roy. Soc. (London) A208, 391.

LONDON, Fritz 1950, Superfluids, vol. I, John Wiley and Sons, Inc. (New York).

LONDON, F. and H. London 1935 Proc. Roy. Soc. (London) A149, 71.

LYNTON, E. A. 1969, Superconductivity, Methuen and Co., Ltd. (London).

MATTHIAS, Bernd 1960, J. Appl. Phys. 31, 23S.

McCUMBER, D. E. 1968, J. Appl. Phys. 39, 3113.

MEIKLEJOHN, W. H. 1964, Rev. Mod. Phys. 36, 302.

MEISSNER, Hans 1958, Phys. Rev. 109, 686.

MEISSNER, Hans 1960, Phys. Rev. 117, 672.

NBS 1961, A Compendium of the Properties of Materials at Low Temperatures, phase II, National Bureau of Standards, Boulder, Colorado, Richard B. Stewart and Victor J. Johnson, general editors, WADD technical report 60-56 part IV, Aeronautical Systems Division, Air Force Systems Command, United States Air Force, Wright-Patterson Air Force Base, Ohio.

NOTARYS, H. A. 1971, private communication.

NOTARYS, H. A. and J. E. Mercereau 1969, International Conference on Science of Superconductivity, Stanford, Palo Alto, California (August, 1969).

PARKS, R. D. and W. A. Little 1964, Phys. Rev. 133, A97.

SCHMID, Albert 1969, Journal of Low Temperature Physics 1, 13.

SIMMONS, W. A. and D. H. Douglass, Jr. 1962, Phys. Rev. Letters 9, 153.

SMITH, Paul H., Sidney Shapiro, John L. Miles and James Nicol 1961, Phys. Rev. Letters 6, 686.

SONDHEIMER, E. H. 1952, Advances in Physics, 1, 1.

STEWART, W. C. 1968, Appl. Phys. Letters 12, 277.

STRNAD, A. R., C. F. Hempstead and Y. B. Kim 1964 Phys. Rev. Letters 13, 794.

TINKHAM, M. 1964 Phys. Rev. Letters 13, 804.

TOWNES, C. H. and J. Turkevich 1950, Phys. Rev. 77, 148.

VOLGER, F. A., A. C. Staas and Van Vijfeijken 1964, Phys. Letters 9, 303.

WEBB, W. W. and R. J. Warburton 1968, Phys. Rev. Letters 20, 461.

YU, M. L. 1971, private communication.

ZIMMERMAN, J. E. and A. H. Silver 1964, Phys. Letters 10, 47.

ZIMMERMAN, J. E. and A. H. Silver 1966, Phys. Rev. 141, 367.